

# Floquet engineering of classical systems

Sho Higashikawa,<sup>1</sup> Hiroyuki Fujita,<sup>2</sup> and Masahiro Sato<sup>3</sup>

<sup>1</sup>*Department of Physics, University of Tokyo, Hongo 113-8656, Japan\**

<sup>2</sup>*Institute for Solid State Physics, University of Tokyo, Kashiwa 277-8581, Japan<sup>†</sup>*

<sup>3</sup>*Department of Physics, Ibaraki University, Mito, Ibaraki 310-8512, Japan<sup>‡</sup>*

(Dated: February 15, 2022)

We derive a systematic high-frequency expansion for the equations of motion of both closed and open classical systems under a periodic drive. For classical systems, known approaches based on the Floquet theorem fail due to the nonlinearity in equations of motion (EOMs) in contrast to quantum systems. Here, employing a master-equation approach, we overcome this difficulty, successfully extending the Floquet methodology to classical EOMs to obtain their high-frequency expansions. Our method is applicable to a broad class of classical and quantum systems described by nonlinear stochastic differential equations including the Langevin equation, the Gross-Pitaevskii equation, the time-dependent Ginzburg-Landau equation, and the stochastic Landau-Lifshitz-Gilbert (sLLG) equation. We illustrate our method by examples of the Kapitza pendulum with friction and laser-driven magnets described by the sLLG equation, confirming that the effective EOMs obtained from their high-frequency expansions well approximate the original time-dependent EOMs. Remarkably, the former EOMs are found to agree well with the latter ones not only in a short time but also for a long time up to the non-equilibrium steady states. This agreement indicates that the high-frequency expansion for a classical dissipative system is, at least asymptotically, convergent in stark contrast to that for an isolated system, provided that the dissipation is sufficiently strong. In the example of driven magnets, we demonstrate the controlled generations of a macroscopic magnetization and a spin chirality by laser and discuss possible applications to spintronics.

## I. INTRODUCTION

Thanks to the rapid developments in laser and ultrafast spectroscopy techniques, recent years had witnessed a remarkable progress in the studies of periodically driven quantum systems in solid-state, atomic, and molecular physics [1–4], where a number of far-from-equilibrium phenomena are investigated; Higgs mode in superconductors [5–7], dynamical localization [8, 9], and coherent destruction of tunneling [10, 11], to name a few. Moreover, a periodic drive is found to be a new versatile tool for engineering quantum systems. This form of quantum engineering, usually termed *Floquet engineering*, is based on the fact that the time evolution of a periodically driven quantum system is effectively described by a time-independent *effective Hamiltonian* thanks to the Floquet theorem [12], a temporal analog of the Bloch theorem. The Floquet engineering enables us to propose and realize various non-equilibrium phenomena including the dynamic control of the superfluid-insulator transition [13–15], the creation of artificial gauge fields [16–19], the implementation of frustrated magnets [20–22], Floquet topological insulators [23–28], and the control of a magnetization, a spin chirality, and a spin-liquid state [29–33].

For a fast drive, the analysis of the effective Hamiltonian is simplified by a systematic high-frequency expansion called the *Floquet-Magnus* (FM) expansion [34–

38]. Although the FM expansion is, in general, a divergent series, its truncated series well describes the dynamics of an isolated quantum system in an intermediate time domain before heating up, known as the Floquet-prethermal regime [37–39]. It is widely believed that the divergent nature of the FM expansion is generic to non-integrable quantum many-body systems as it indicates eventual heating to a featureless infinite-temperature state due to persistent driving [27, 40–44]. It is recently shown that an isolated classical spin system under a fast periodic drive also exhibits the Floquet prethermalization similarly to quantum systems [45, 46], indicating the possibility of extending the Floquet methodology to classical systems.

While remarkable progress has been made concerning quantum systems for a past few decades, periodically driven *classical* systems have a long history of study, where a number of interesting phenomena are found such as dynamical localization [47], stochastic resonance [48, 49], and dynamical stabilization [50–55]. Thus, it is clearly essential to extend the Floquet methodology established in quantum systems to classical ones, in particular, to develop a general framework for obtaining the high-frequency expansion of their EOMs. In fact, such generalizations have a wide range of application not only from purely classical systems, e.g., a Langevin system in biology and chemistry [56], but also quantum systems in symmetry broken phases, e.g., Bose-Einstein condensates described by the Gross-Pitaevskii equation [57, 58], micromagnets described by the Landau-Lifshitz-Gilbert (LLG) equation [59–61], and generic ordered phases following the time-dependent Ginzburg-Landau equation. Also, it is desirable to generalize to *open* classical sys-

\* higashikawa@cat.phys.s.u-tokyo.ac.jp

† h-fujita@issp.u-tokyo.ac.jp

‡ masahiro.sato.phys@vc.ibaraki.ac.jp

tems for practical application to, e.g., biology and solid-state physics. As emphasized in the studies on the Floquet engineering of quantum systems [10, 62–70], the coupling with an environment is essential for preventing the system from heating up due to the driving. However, the generalization to classical EOMs is so far limited to Hamilton systems [40, 46] or rely on some variational state [54, 55, 71]. One difficulty is that the Floquet theorem, which is the heart of the Floquet engineering, can be applied to only linear differential equations like Schrödinger equation [2, 12], while classical systems are, in general, described by nonlinear EOMs. Another difficulty arises in open classical systems. When a system is coupled to a thermal bath, the thermal fluctuation appears in its EOM as a stochastic variable and breaks the strict periodicity of the EOM, which again makes the applicability of the Floquet theorem unclear.

In this paper, we develop a systematic high-frequency expansion for a periodically driven classical system that is applicable to both closed and open systems coupled to a thermal reservoir. The key idea is using, the corresponding master equations [72] to its EOM, rather than its EOM itself. Since the master equations are linear in the probability distribution function and periodic with time, one can safely apply the Floquet theorem. The effective EOM is derived from the FM expansion of the master equation through the correspondence between the EOM and the master equation. We illustrate this method by two open classical systems: (i) the Kapitza pendulum [50] with friction, (ii) laser-irradiated magnets described by the stochastic LLG (sLLG) equation, where we compare the original time-dependent EOMs and the effective EOMs obtained from the high-frequency expansion. In both cases, we confirm that the effective ones well approximate the short-time dynamics of the time-dependent ones. Moreover, the effective ones are found to correctly describe the long-time dynamics until the non-equilibrium steady state (NESS), in stark contrast to closed quantum systems where the truncated FM expansion fails to capture the eventual heating to infinite temperature [2, 37–39, 43]. This result indicates that the FM expansion for a classical driven dissipative system is a convergent series due to the suppression of the heating through the coupling with a thermal reservoir. Finally, we also present an application to spintronics [73], where we analyze a multiferroic spin chain irradiated by a circularly polarized laser. We show that a synthetic Dzyaloshinskii-Moriya (DM) interaction [74, 75] emerges, leading to a spiral magnetic order in the NESS.

The rest of this paper is organized as follows. In Sec. II, we present the general formalism on the FM expansion of a classical EOM with and without a stochastic variable. In Sec. III and IV, we illustrate our method by considering a single particle system, the Kapitza pendulum with friction, and a many-body system, the periodically driven sLLG equation, respectively, and compare the time-periodic EOM and their effective EOM obtained by their FM expansion. In Sec. V, we present an appli-

cation to spintronics, where we study a multiferroic spin chain irradiated by a laser. In Sec. VI, we summarize the main results and discuss the outlook for future studies.

## II. FM EXPANSION OF A CLASSICAL (STOCHASTIC) EQUATION OF MOTION

### A. Equation of motion and master equation

Consider a classical system under a periodic drive. Let  $\phi(t) = [\phi_1(t), \phi_2(t), \dots, \phi_N(t)]$  be a set of classical variables describing the system, e.g., a position of a particle for the Langevin equation and a magnetization for the sLLG equation, where  $t$  represents the time. We consider the system described by the following stochastic differential equation [76]:

$$\dot{\phi}_i(t) = f_i[\phi(t), t] + \sum_{j=1}^N g_{ij}[\phi(t), t] h_j(t), \quad (1)$$

where  $\dot{y} := dy/dt$  is the time derivative and  $h_j$  is a Gaussian random variables satisfying

$$\begin{aligned} \langle h_i(t) \rangle &= 0, \\ \langle h_i(t) h_j(t') \rangle &= 2D \delta_{ij} \delta(t - t'), \end{aligned} \quad (2)$$

with  $D$  being the diffusion constant. The drift force  $f_i(\phi, t)$  and the diffusion matrix  $g_{ij}(\phi, t)$  are time-periodic with period  $T$ :  $f_i(\phi, t+T) = f_i(\phi, t)$  and  $g_{ij}(\phi, t+T) = g_{ij}(\phi, t)$ , and they are, in general, non-linear functions of  $\phi$ . We note that when we consider an EOM for a classical field  $\phi_{\mathbf{r}} = [\phi_{\mathbf{r},1}(t), \phi_{\mathbf{r},2}(t), \dots, \phi_{\mathbf{r},N_I}(t)]$ , the subscript  $i$  in Eq. (1) represents a collection of the coordinate  $\mathbf{r}$  and the internal degrees of freedom  $a$ , where the EOM is written as follows:

$$\dot{\phi}_{\mathbf{r},a}(t) = f_{\mathbf{r},a}[\phi(t), t] + \sum_{b=1}^{N_I} g_{\mathbf{r},ab}[\phi(t), t] h_{\mathbf{r},b}(t). \quad (3)$$

We assume that the effect of the random field is local, i.e., the field  $\phi_{\mathbf{r}}$  at  $\mathbf{r}$  is affected by the random field  $h_{\mathbf{r}}$  at  $\mathbf{r}$ . We here chose the Stratonovich prescription for the application to the sLLG equation in Sec. IV since the magnetization is conserved only for this prescription [77]. However, a generalization of the following theory to the other prescriptions is straightforward [76].

Equations (1) and (3) with finite diffusion  $D > 0$  are commonly used to describe diffusive processes in nature, such as a Langevin motion [56] and spin dynamics of a micromagnet [61]. For the overdamped Langevin equation in the one-dimensional space with the potential  $U(x)$  and the mobility  $\mu$ , its EOM reads

$$\dot{x} = -\mu \frac{\partial U(x)}{\partial x} + h(t), \quad (4)$$

where  $\phi = x$  and  $\mathbf{f} = -\mu \partial U(x)/(\partial x)$  are the position of the particle and the potential force, respectively, and  $g_{ij} = 1$ . When  $D = 0$ , Eq.(1) gives a deterministic equation

$$\dot{\phi}_i(t) = f_i[\phi(t), t], \quad (5)$$

describing an open classical system at sufficiently low temperature or a closed classical system such as a Hamilton system.

In addition to classical systems, our theory can be applied to even *quantum* systems in symmetry-broken phases or the semiclassical regime because their EOMs takes the form of Eq. (1). In the former case,  $\phi$  and Eq. (1) are the order parameter and its equation, e.g., the Gross-Pitaevskii (GP) equation [57, 58] and the Ginzburg-Landau equation [78], respectively. For the GP equation, the order parameter  $\phi = \{\psi_{\mathbf{r}}\}_{\mathbf{r} \in \mathbb{R}^3}$  represents the macroscopic wavefunction, with its equation written into the form of Eq. (1) with  $D = 0$ :

$$\dot{\psi}_{\mathbf{r}} = -i \left[ -\frac{\nabla_{\mathbf{r}}^2 \psi_{\mathbf{r}}}{2m} + (\mu + g_c |\psi_{\mathbf{r}}|^2) \psi_{\mathbf{r}} \right]. \quad (6)$$

Here,  $m$ ,  $\mu$  and  $g_c$  being the mass of atoms, the chemical potential and the coupling constant, respectively. An example of the latter case is the Dicke model in the semiclassical limit [79, 80], which describes two-level atoms coupled to a large number of photons in a cavity. In this limit, the system is described by the effective collective atomic pseudospin  $\mathbf{J} := (J_x, J_y, J_z)$ , which is a classical three-component vector, and the coherent-state amplitude  $a$  of the photons, which is a complex number. Its EOM is given from the Ehrenfest equation  $d\langle A \rangle/dt = id\langle [H, A] \rangle$  as follows:

$$\begin{aligned} \dot{\mathbf{J}} &= (2\lambda \text{Re}(a) \hat{x} + \omega_a \hat{z}) \times \mathbf{J}, \\ \dot{a} &= -i(\omega_o a + \lambda J_x), \end{aligned} \quad (7)$$

where  $\omega_a, \omega_o$ , and  $\lambda$  is the atomic frequency, the optical frequency, and the coupling constant between the photons and atoms, respectively, and  $\hat{x} := (1, 0, 0)$  and  $\hat{z} := (0, 0, 1)$ .

By introducing the vector fields  $\mathbf{f} := (f_1, f_2, \dots, f_N)$  and  $\mathbf{h} := (h_1, h_2, \dots, h_N)$ , and the matrix-valued function  $G := \{g_{ij}\}_{i,j=1}^N$ , we can rewrite Eqs.(1) and (2) in compact forms:

$$\begin{aligned} \dot{\phi} &= \mathbf{f}(\phi, t) + G(\phi, t)\mathbf{h}(t), \\ \langle \mathbf{h}(t) \rangle &= 0, \\ \left\langle [\mathbf{h}(t)]^{\text{tr}} \mathbf{h}(t') \right\rangle &= 2DI_N \delta(t - t'), \end{aligned} \quad (8)$$

where the superscript tr denotes the transpose. Using the standard technique of the stochastic calculus [61, 77, 81, 82], we obtain the master equation (Fokker-Planck

equation) corresponding to Eq.(1):

$$\begin{aligned} \frac{\partial P(\phi, t)}{\partial t} &= \frac{\partial}{\partial \phi_i} [\mathcal{F}_i(\phi, t)P(\phi, t)] \\ &+ \frac{\partial^2}{\partial \phi_i \partial \phi_j} [\mathcal{D}_{ij}(\phi, t)P(\phi, t)], \end{aligned} \quad (9)$$

where

$$\begin{aligned} \mathcal{F}_i(\phi, t) &:= -f_i(\phi, t) - Dg_{kl}(\phi, t) \frac{\partial g_{il}(\phi, t)}{\partial \phi_k}, \\ \mathcal{D}_{ij}(\phi, t) &:= Dg_{ik}(\phi, t)g_{jk}(\phi, t). \end{aligned} \quad (10)$$

Here,  $P(\phi', t)$  is the probability density for finding the variable  $\phi = \phi'$  at time  $t$  in the whole parameter space of  $\phi$ , and we omit the summation of the repeated indices  $i, j, k, l$ . Equations (8), (9), (10) give the correspondence between the EOM and the master equation. By introducing the current  $J_i := -\mathcal{F}_i P - \partial(D_{ij}P)/(\partial \phi_j)$ , we can rewrite Eq.(9) into the continuity equation for  $P$ :

$$\partial_t P + \text{div} \mathbf{J} = 0, \quad (11)$$

where  $\text{div} \mathbf{J} := \sum_i \partial J_i / \partial \phi_i$ . This equation satisfies the conservation of the probability:  $\int d\phi P(\phi, t) = 1$  for  $\forall t$ . We note that the master equation (9) contains only up to the second order derivative of  $\phi$  because the random variable  $\mathbf{h}$  is Markovian and Gaussian. In other words, if the master equation contains higher-order derivative or becomes an integro-differential equation, the random noise must be either non-Markovian or non-Gaussian [83–87]. We will again comment on this issue in the next subsection.

If we introduce the vector field  $\mathcal{F} := (\mathcal{F}_1, \mathcal{F}_2, \dots, \mathcal{F}_N)$  and the matrix-valued field  $\mathcal{D} := \{\mathcal{D}_{ij}\}_{i,j=1}^N$ , Eq.(9) can be rewritten in a compact form:

$$\partial_t P(\phi, t) = \text{div}(\mathcal{F}P) + \text{div}_2(\mathcal{D}P), \quad (12)$$

where the operator  $\text{div}_2$  on a matrix  $\mathcal{D}' = \{\mathcal{D}'_{ij}(\phi)\}_{i,j}$  is defined by  $\text{div}_2(\mathcal{D}') := (\partial^2 \mathcal{D}'_{ij})/(\partial \phi_i \partial \phi_j)$ .

## B. FM expansion of a master equation

In an analysis of a driven quantum system, Floquet theorem [12] and the high-frequency expansion [2] are commonly used techniques, since they allow us to map a non-equilibrium system to an effective static system and hence greatly simplify its analysis. Unfortunately, we cannot apply them directly to classical EOMs because the original equation (1) is neither linear in  $\phi$  nor time-periodic due to the random variable  $h_j(t)$ . Nevertheless, we can apply it to its master equation (9) because it is linear in  $P$  and time-periodic. Figure 1 summarizes our strategy. The FM expansion of an EOM is performed via that of a master equation.

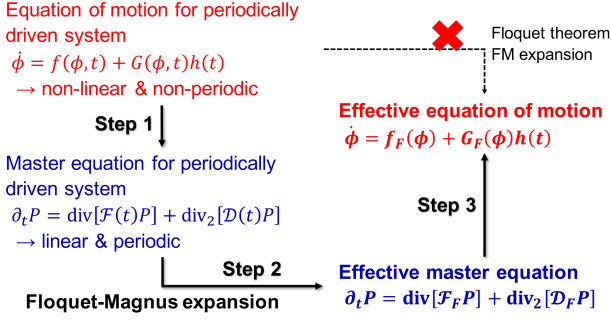


FIG. 1. Procedure for obtaining the FM expansion of the classical EOM described by the ordinary stochastic differential equation (1). In the first step, we turn to the master equation (9) corresponding to Eq. (1), where we perform the FM expansion to obtain the effective master equation (20) in the second step. Finally, we find an ordinary stochastic differential equation corresponding to the effective master equation.

By introducing the Fokker-Planck operator  $\mathcal{L}_t$  defined by

$$\mathcal{L}_t(P) = \text{div}[\mathcal{F}(t)P] + \text{div}_2[\mathcal{D}(t)P], \quad (13)$$

we can regard Eq. (9) as the “Schrödinger equation” driven by the non-Hermitian time-periodic “Hamiltonian”  $H(t) := i\mathcal{L}_t$  [88]:

$$i\partial_t P = H(t)P, \quad (14)$$

where the probability distribution  $P$  plays the role of a wave function. We can formally solve Eq. (14) as  $P(\phi, t) = U(t, 0)P(\phi, t = 0)$ , where  $U(t_2, t_1)$  is the time evolution operator from  $t_1$  to  $t_2$ . From the Floquet theorem, we can rewrite  $U(t_2, t_1)$  using the effective Hamiltonian  $H_F$  and the micromotion operator  $U_F^\pm(s) := \exp[\pm\mathcal{G}_F(s)]$  as follows [2, 36]:

$$\begin{aligned} U(t_2, t_1) &:= \mathcal{T}_t \exp\left[-i \int_{t_1}^{t_2} H(t)dt\right] \\ &= U_F^+(t_2) e^{-i(t_2-t_1)H_F} U_F^-(t_1) \\ &= e^{\mathcal{G}_F(t_2)} e^{(t_2-t_1)\mathcal{L}_F} e^{-\mathcal{G}_F(t_1)}, \end{aligned} \quad (15)$$

where  $\mathcal{T}_t$  is the time ordering operator. In the last line, we introduce the effective Fokker-Planck operator  $\mathcal{L}_F := -iH_F$ . In the context of quantum systems,  $i\mathcal{G}_F(s)$  is called the “kick” operator [34] and satisfies the time-periodicity  $\mathcal{G}_F(s+T) = \mathcal{G}_F(s)$ , representing an instantaneous time evolution at time  $s$  and induces a small oscillational motion around the slower dynamics. In what follows, we call  $\mathcal{G}_F(t)$  itself the kick operator as well. Note that the Floquet theorem itself does not require the Hermiticity of  $H(t)$  and hence apply to the above non-Hermitian Schrödinger equation.

For a fast drive, the effective Fokker-Planck operator  $\mathcal{L}_F$  as well as the micromotion operator  $U_F$  can be approximated by their truncated FM expansions  $\mathcal{L}_F :=$

$\sum_{m=0}^{m_0} \mathcal{L}_F^{(m)}$  and  $U_F(t) := \exp\left[\sum_{m=0}^{m_0} \mathcal{G}_F^{(m)}(t)\right]$ , respectively [34, 89, 90], up to some truncation order  $m_0$ , with  $\mathcal{L}_F^{(m)}$  and  $\mathcal{G}_F^{(m)}$  being the  $m$ th-order terms. As we will show below,  $\mathcal{L}_F^{(m)}$  and  $\mathcal{G}_F^{(m)}$  are derived in the same manner as those in quantum cases [34, 36].

Let us expand  $\mathcal{L}_t$  and  $H(t)$  in their Fourier harmonics as follows:

$$\begin{aligned} \mathcal{L}_t &= \sum_m \mathcal{L}_m e^{-im\omega t}, \\ H(t) &= \sum_m H_m e^{-im\omega t}, \end{aligned} \quad (16)$$

where  $\mathcal{L}_m = -iH_m$ . Conversely,  $\mathcal{L}_m$  ( $H_m$ ) is determined from  $\mathcal{L}_t$  ( $H(t)$ ) as  $\mathcal{L}_m = \frac{1}{T} \int_0^T dt \mathcal{L}_t e^{im\omega t}$  ( $H_m = \frac{1}{T} \int_0^T dt H(t) e^{im\omega t}$ ). Up to the second-order,  $\mathcal{L}_F^{(m)}$  is expressed as follows [34, 36]:

$$\begin{aligned} \mathcal{L}_F^{(0)} &= -iH_F^{(0)} = -iH_0 = \mathcal{L}_0, \\ \mathcal{L}_F^{(1)} &= -iH_F^{(1)} = -i \sum_{m \neq 0} \frac{[H_{-m}, H_m]}{2m\omega}, \\ &= i \sum_{m \neq 0} \frac{[\mathcal{L}_{-m}, \mathcal{L}_m]}{2m\omega}, \\ \mathcal{L}_F^{(2)} &= -iH_F^{(2)} \\ &= -i \sum_{m \neq 0} \left\{ \frac{[H_{-m}, [H_0, H_m]]}{2(m\omega)^2} \right. \\ &\quad \left. + \sum_{m' \neq 0, m} \frac{[H_{-m'}, [H_{m'-m}, H_m]]}{3mm'\omega^2} \right\}, \\ &= i^2 \sum_{m \neq 0} \left\{ \frac{[\mathcal{L}_{-m}, [\mathcal{L}_0, \mathcal{L}_m]]}{2(m\omega)^2} \right. \\ &\quad \left. + \sum_{m' \neq 0, m} \frac{[\mathcal{L}_{-m'}, [\mathcal{L}_{m'-m}, \mathcal{L}_m]]}{3mm'\omega^2} \right\}, \end{aligned} \quad (17)$$

where the kick operator  $\mathcal{G}_F^{(m)}$  is given by

$$\begin{aligned} \mathcal{G}_F^{(0)}(t) &= 0, \\ \mathcal{G}_F^{(1)}(t) &= - \sum_{m \neq 0} \frac{H_{-m} e^{im\omega t}}{m\omega} = -i \sum_{m \neq 0} \frac{\mathcal{L}_{-m} e^{im\omega t}}{m\omega}, \\ \mathcal{G}_F^{(2)}(t) &= \sum_{m \neq 0} \left\{ \frac{[H_0, H_{-m}] e^{im\omega t}}{(m\omega)^2} \right. \\ &\quad \left. + \sum_{m' \neq 0, m} \frac{[H_{m'}, H_{-m}] e^{i(m-m')\omega t}}{2m(m-m')\omega^2} \right\} \\ &= i^2 \sum_{m \neq 0} \left\{ \frac{[\mathcal{L}_0, \mathcal{L}_{-m}] e^{im\omega t}}{(m\omega)^2} \right. \\ &\quad \left. + \sum_{m' \neq 0, m} \frac{[\mathcal{L}_{m'}, \mathcal{L}_{-m}] e^{i(m-m')\omega t}}{2m(m-m')\omega^2} \right\}. \end{aligned} \quad (18)$$

We note that the commutator  $[\cdot, \cdot]$  in Eqs. (17) and (18) is interpreted as that between operators:

$$[\mathcal{S}_1, \mathcal{S}_2](P) := \mathcal{S}_1[\mathcal{S}_2(P)] - \mathcal{S}_2[\mathcal{S}_1(P)]. \quad (19)$$

We further note that we have taken the convention  $\int_0^T \mathcal{G}_F(t) dt = 0$  such that the effective Fokker-Planck operator becomes time-independent. In this convention,  $\mathcal{G}_F$  and  $\mathcal{L}_F$  are the same as those obtained from the van-Vleck degenerate perturbation theory [2, 36, 91]. In summary, the effective Fokker-Planck operator  $\mathcal{L}_F^{(m)}$  is obtained by formally replacing the  $m$ th coefficient  $H_m$  of the Hamiltonian by of the Fokker-Planck operator  $\mathcal{L}_m$  and the commutators between the Hamiltonians by the commutator (19), and finally multiplying  $i^m$ . If we focus on the effective dynamics ignoring the micromotion, the master equation is given by the following time-independent equation of motion

$$\partial_t P = \mathcal{L}_F P = \sum_{m=0}^{m_0} \mathcal{L}_F^{(m)} P. \quad (20)$$

So far, our argument has focused only on the FM expansion. However, it is straightforward to generalize our analysis to other expansions like the Brillouin-Wigner expansion [92] and the Floquet-Schrieffer-Wolff transformation [33, 93–95].

To complete the procedure in Fig. 1, we must find an EOM whose master equation coincides with the truncated effective master equation obtained from the FM expansion (the step 3 in Fig. 1). In general, this problem is nontrivial. For a Markovian random variable  $h_j$  with Gaussian correlation, the master equation includes at most the second-order derivative terms  $\partial^2(\mathcal{D}_{ij}P)/(\partial\phi_i\partial\phi_j)$  [72]. In other words, when the truncated FM expansion of a master equation contains derivatives higher than the second-order, e.g.,  $\partial^3(\tilde{\mathcal{D}}_{ijk}P)/(\partial\phi_i\partial\phi_j\partial\phi_k)$ , the random variable  $h_j$  must be either non-Markovian or non-Gaussian [83–87]. In fact, for the case a quantum master equation under a periodic drive, non-Markov nature appear in the effective equation, which is well-captured by introducing a memory kernel [96]. It is unclear where one can construct a similar memory kernel or correlation functions of a random variable for a given master equation, though approximation methods are developed [72, 97]. Nevertheless, as we will see below, we can find the corresponding EOM for several physically relevant situations including the case where the diffusion vanishes:  $\mathcal{D} = 0$ , or is time-independent:  $\mathcal{D}(t) = \text{const}$ .

### C. Deterministic system

We here consider the system without diffusions, i.e., without random fields:  $\mathcal{D} = 0$  and  $h_j(t) = 0$ . In this case, its EOM  $\dot{\phi} = \mathbf{f}(\phi, t)$  can be regarded as a flow equation generated by  $\mathbf{f}(\phi, t)$ . Then,  $\mathcal{L}_m$  is written as

$\mathcal{L}_m(P) := -\text{div}(\mathbf{f}_m P)$ , and the commutator  $[\mathcal{L}_m, \mathcal{L}_n]$  is given by

$$\begin{aligned} [\mathcal{L}_m, \mathcal{L}_n](P) &= \text{div}[\mathbf{f}_m \text{div}(\mathbf{f}_n P)] - \text{div}[\mathbf{f}_n \text{div}(\mathbf{f}_m P)] \\ &= \text{div}\{[(\mathbf{f}_m \cdot \nabla_\phi) \mathbf{f}_n - (\mathbf{f}_n \cdot \nabla_\phi) \mathbf{f}_m] P\} \\ &= -\text{div}(-[\mathbf{f}_m, \mathbf{f}_n]_{\text{cl}} P). \end{aligned} \quad (21)$$

Here  $\nabla_\phi := (\partial/\partial\phi_1, \partial/\partial\phi_2, \dots)$ , and the commutator  $[\mathbf{A}, \mathbf{B}]_{\text{cl}}$  between two vector fields  $\mathbf{A}$  and  $\mathbf{B}$  is defined by

$$\begin{aligned} [\mathbf{A}, \mathbf{B}]_{\text{cl},j} &= (\mathbf{A} \cdot \nabla_\phi) B_j - (\mathbf{B} \cdot \nabla_\phi) A_j \\ &:= A_i \frac{\partial B_j}{\partial \phi_i} - B_i \frac{\partial A_j}{\partial \phi_i}, \end{aligned} \quad (22)$$

which is called the Lie bracket in mathematics. Equation (21) implies that the operators of the form  $\mathcal{L} := \text{div}(\mathbf{f} \cdot)$  is closed with respect to the commutator, and thereby the effective dynamics is described by the renormalized drift force  $\mathbf{f}_F$ . The  $m$ th order FM expansion  $\mathbf{f}_F^{(m)}$  of the drift field is obtained from that  $H_F^{(m)}$  of the effective Hamiltonian by replacing the commutator  $[H_m, H_n]$  between Hamiltonians with that  $[\mathbf{f}_m, \mathbf{f}_n]_{\text{cl}}$  between drift fields, followed by the multiplication of  $i^m$ . Then, the resulting effective EOM is given by

$$\begin{aligned} \dot{\phi} &= \mathbf{f}_F(\phi) \\ &= \mathbf{f}_0(\phi) + i \sum_{m \neq 0} \frac{[\mathbf{f}_{-m}, \mathbf{f}_m]_{\text{cl}}}{2m\omega} \\ &\quad - \sum_{m \neq 0} \left\{ \frac{[\mathbf{f}_{-m}, [\mathbf{f}_0, \mathbf{f}_m]_{\text{cl}}]_{\text{cl}}}{2(m\omega)^2} \right. \\ &\quad \left. + \sum_{m' \neq 0, m} \frac{[\mathbf{f}_{-m'}, [\mathbf{f}_{m'-m}, \mathbf{f}_m]_{\text{cl}}]_{\text{cl}}}{3mm'\omega^2} \right\} + \mathcal{O}(\omega^{-3}), \end{aligned} \quad (23)$$

up to the order of  $\omega^{-2}$ . This result is consistent with the Magnus expansion of general non-autonomous (not necessarily time-periodic) ordinary differential equation  $\dot{\phi} = \mathbf{f}(\phi, t)$  [98–101]. As a special case, if the dynamics are governed by some classical Hamiltonian  $H(t)$ , the drift field  $\mathbf{f}(t)$  and the commutator  $[\cdot, \cdot]_{\text{cl}}$  are replaced by the Hamilton flow and the Poisson bracket  $-\{\cdot, \cdot\}$ , respectively. Note that the master equation (9) is nothing but the Liouville equation. Let  $\mathbf{q}$  and  $\mathbf{p}$  be a canonical conjugate pair. Then, the classical variable  $\phi$  and  $\mathbf{f}_m$  are given by

$$\phi = (\mathbf{q}, \mathbf{p}), \quad \mathbf{f}_m = \left( \frac{\partial H_m}{\partial \mathbf{p}}, -\frac{\partial H_m}{\partial \mathbf{q}} \right). \quad (24)$$

By a straightforward calculation, we obtain

$$[\mathbf{f}_m, \mathbf{f}_n]_{\text{cl}} = - \left( \frac{\partial \{H_m, H_n\}}{\partial \mathbf{p}}, -\frac{\partial \{H_m, H_n\}}{\partial \mathbf{q}} \right). \quad (25)$$

The above results correctly reproduce the previous results for periodically driven isolated Hamilton systems [2, 40, 46] and are consistent with the Magnus expansion of general time-dependent (not necessarily time-periodic) Hamilton systems [102–104].

#### D. Time-independent diffusion

We here assume that the diffusion matrix  $G$  and hence  $\mathcal{D}$  are time-independent, where the  $\mathcal{L}_m$  is given by

$$\begin{aligned}\mathcal{L}_0(P) &:= \text{div}(\mathcal{F}_0 P) + \text{div}_2[DP], \\ \mathcal{L}_m(P) &:= \text{div}(\mathcal{F}_m P) \quad \text{for } m \neq 0,\end{aligned}\quad (26)$$

where  $\mathcal{F}_m$  is the  $m$ th-order Fourier harmonics of  $\mathcal{F}(t)$ . Under this assumption, one can always find the effective EOM corresponding to the effective Fokker-Planck operator  $\mathcal{L}_F$  at least up to the second order of the FM expansion if we truncate in the second order. From Eq. (18), the first order is given by

$$\begin{aligned}\mathcal{L}_F^{(1)} &:= i \sum_{m \neq 0} \frac{[\mathcal{L}_{-m}, \mathcal{L}_m]}{2m\omega} = \text{div}[\mathcal{F}_F^{(1)} \cdot], \\ \mathcal{F}_F^{(1)} &:= \sum_{m \neq 0} \frac{i}{2m\omega} [(\mathcal{F}_{-m} \cdot \nabla_\phi) \mathcal{F}_m - (\mathcal{F}_m \cdot \nabla_\phi) \mathcal{F}_{-m}] \\ &= \sum_{m \neq 0} \frac{i}{2m\omega} [(\mathbf{f}_{-m} \cdot \nabla_\phi) \mathbf{f}_m - (\mathbf{f}_m \cdot \nabla_\phi) \mathbf{f}_{-m}],\end{aligned}\quad (27)$$

where the effective Fokker-Planck operator is given by

$$\mathcal{L}_F(P) = \text{div}[(\mathcal{F}_0 + \mathcal{F}_F^{(1)})P] + \text{div}_2(DP). \quad (28)$$

A crucial observation here is that only the drift field is renormalized in the first order. Therefore, we can always find the EOM with Fokker-Planck operator (28), which is given by

$$\dot{\phi} = \mathbf{f}_F(\phi) + G(\phi)h(t), \quad (29)$$

where  $\mathbf{f}_F$  is the renormalized drift term:

$$\mathbf{f}_F := \mathbf{f}_0 + \sum_{m \neq 0} \frac{i}{2m\omega} [(\mathbf{f}_m \cdot \nabla_\phi) \mathbf{f}_{-m} - (\mathbf{f}_{-m} \cdot \nabla_\phi) \mathbf{f}_m]. \quad (30)$$

Notably, when  $\mathbf{f}_F$  represents a potential force with a renormalized potential  $V_F$  and  $G(\phi)$  satisfies the detailed balance at temperature  $T_{\text{te}}$ , the system goes to a canonical distribution  $\exp(-V_F/T_{\text{te}})$  under the potential  $V_F$ . The time evolution without the micromotion operator is obtained by solving Eq. (30).

On the other hand, the calculation of the time evolution with the micromotion operator is constituted from three steps corresponding to the three exponential operators  $\exp[-\mathcal{G}_F(t_1)]$ ,  $\exp[(t_2 - t_1)\mathcal{L}_F]$ , and  $\exp[\mathcal{G}_F(t_2)]$ , as shown in Eq. (15). Let us first consider the effect of kick operator on the EOM. The kick operator  $\mathcal{G}_F^{(1)}(s)$ , with  $s (= t_1, t_2)$  being either the initial or final kick time, is given from Eq. (18) as

$$\mathcal{G}_F^{(1)}(s) = -\frac{1}{\omega} \text{div}[\tilde{\mathbf{f}}_{F,\text{mic}}^{(1)}(\phi, s) \cdot], \quad (31)$$

where  $\tilde{\mathbf{f}}_{F,\text{mic}}^{(1)}$  is the oscillating drift field:

$$\tilde{\mathbf{f}}_{F,\text{mic}}^{(1)}(\phi, s) = -i \sum_{m \neq 0} \frac{\mathbf{f}_{-m} e^{i\omega s}}{2m}. \quad (32)$$

From Eq. (32) and the definition of an exponential operator,  $\exp[\pm\mathcal{G}_F(s)]P_0(\phi)$  is formally the solution of the master equation

$$\begin{aligned}\frac{\partial P(\phi, \tau)}{\partial \tau} &= \mp \text{div}[\tilde{\mathbf{f}}_{F,\text{mic}}^{(1)}(\phi, s)P(\phi, \tau)], \\ P(\phi, \tau = 0) &= P_0(\phi),\end{aligned}\quad (33)$$

at time  $\tau = 1/\omega$ . Thus, the exponential  $\exp[\pm\mathcal{G}_F(s)]$  has the following physical interpretation: it is the integration of the flow field  $\tilde{\mathbf{f}}_{F,\text{mic}}^{(1)}$  from  $\tau = 0$  to  $\tau = 1/\omega$ , where  $\tau$  is the auxiliary time for calculating the kicks and  $1/\omega$  is the duration of the kick. Since the above equation does not contain the diffusion term, plugging  $P_0(\phi_{\text{kick}}) = \delta(\phi_{\text{kick}} - \phi_0)$  into Eq.(33), we rewrite it into the equation for  $\phi_{\text{kick}}$ :

$$\frac{d\phi_{\text{kick}}}{d\tau} = \pm \tilde{\mathbf{f}}_{F,\text{mic}}^{(1)}(\phi_{\text{kick}}, s), \quad \phi_{\text{kick}}(\tau = 0) = \phi_0. \quad (34)$$

Thus,  $\phi_0$  is mapped to the solution of Eq. (34) at time  $\tau = 1/\omega$  by the micromotion operator  $\exp[\pm\mathcal{G}_F(s)]$ . Note that Eqs.(33) and (34) are autonomous equations, i.e., not explicitly depend on the time  $t$ . Practically, the solution  $\phi_{\text{kick}}(t = 1/\omega)$  is well approximated by the Euler method:

$$\phi_{\text{kick}}\left(t = \frac{1}{\omega}\right) \simeq \phi_0 \pm \frac{\tilde{\mathbf{f}}_{F,\text{mic}}^{(1)}(\phi_0, s)}{\omega}, \quad (35)$$

from the smallness of the integration time  $1/\omega$ .

We now see the generic effect of the kick operator, and then the three-step computation of the time evolution operator  $U(t_2, t_1) = e^{\mathcal{G}_F(t_2)} e^{(t_2 - t_1)\mathcal{L}_F} e^{-\mathcal{G}_F(t_1)}$  is as follows: Let  $\phi_0$  be the initial state of  $\phi$ . First, to calculate the effect of the initial kick  $\exp[-\mathcal{G}_F(t_1)]$ , we integrate Eq. (34) with minus sign on the right-hand side and  $s = t_1$  for initial condition  $\phi_0$ :

$$\frac{d\phi_{\text{kick}}}{d\tau} = -\tilde{\mathbf{f}}_{F,\text{mic}}^{(1)}(\phi_{\text{kick}}, t_1), \quad \phi_{\text{kick}}(\tau = 0) = \phi_0. \quad (36)$$

The solution at time  $\tau = 1/\omega$  gives the state after the initial kick, which we write as  $\phi_1$ :  $\phi_1 := \phi_{\text{kick}}(\tau = 1/\omega)$ . Next, we evaluate the effective dynamics  $\exp[(t_2 - t_1)\mathcal{L}_F]$  by integrating Eq. (30) from within time  $(t_2 - t_1)$  with initial state is taken as  $\phi_1$ :

$$\frac{d\phi}{dt} = \mathbf{f}_F(\phi) + G(\phi)h(t), \quad \phi(t = 0) = \phi_1. \quad (37)$$

The solution at  $t = t_2 - t_1$  gives the state after the effective flow  $\mathcal{L}_F$ , which we write as  $\phi_2$ :  $\phi_2 := \phi(t = t_2 - t_1)$ .

Finally, we integrate Eq. (34) with plus sign on the right-hand side and  $s = t_2$  up to time  $1/\omega$  for initial condition  $\phi_2$ , calculating the final kick  $\exp[\mathcal{G}_F(t_2)]$ :

$$\frac{d\phi_{\text{kick}}}{d\tau} = \tilde{\mathbf{f}}_{F,\text{mic}}^{(1)}(\phi_{\text{kick}}, t_2), \quad \phi_{\text{kick}}(\tau = 0) = \phi_2. \quad (38)$$

Then, the solution  $\phi_3 = \phi_{\text{kick}}(\tau = 1/\omega)$  gives the state after the final kick, and hence the state applied by the three operators  $e^{-\mathcal{G}_F(t_1)}$ ,  $e^{(t_2-t_1)\mathcal{L}_F}$ , and  $e^{\mathcal{G}_F(t_2)}$  to the initial state  $\phi_0$ .

In the calculation of the second order, there appears the commutator between  $\mathcal{L}(P) = \text{div}(\mathcal{F}P) + \text{div}_2(\mathcal{D}P)$  and  $\mathcal{L}'(P) = \text{div}(\mathcal{F}'P)$ , which is calculated as follows:

$$\begin{aligned} & [\mathcal{L}, \mathcal{L}'](P) \\ &= \text{div}[\mathcal{F}\text{div}(\mathcal{F}'P)] - \text{div}[\mathcal{F}'\text{div}(\mathcal{F}P)] \\ & \quad + \text{div}_2[\mathcal{D}\text{div}(\mathcal{F}'P)] - \text{div}_2[\mathcal{F}'\text{div}_2(\mathcal{D}P)] \\ &=: \text{div}[\text{drf}(\mathcal{F}, \mathcal{F}', \mathcal{D})P] + \text{div}_2[\text{diff}(\mathcal{F}', \mathcal{D})P], \end{aligned} \quad (39)$$

where the corresponding drift field  $\text{drf}(\mathcal{F}, \mathcal{F}', \mathcal{D}) := \{\text{drf}_i(\mathcal{F}, \mathcal{F}', \mathcal{D})\}_{i=1}^N$  and the diffusion matrix  $\text{diff}(\mathcal{F}', \mathcal{D}) = \{\text{diff}_{ij}(\mathcal{F}', \mathcal{D})\}_{i,j=1}^N$  are given by

$$\begin{aligned} \text{drf}_i(\mathcal{F}, \mathcal{F}', \mathcal{D}) &= (\mathcal{F} \cdot \nabla_\phi) \mathcal{F}'_i - (\mathcal{F}' \cdot \nabla_\phi) \mathcal{F}_i - \frac{\partial^2 \mathcal{F}'_i}{\partial \phi_j \partial \phi_k} \mathcal{D}_{jk}, \\ \text{diff}_{ij}(\mathcal{F}', \mathcal{D}) &= \frac{\partial \mathcal{F}'_i}{\partial \phi_k} \mathcal{D}_{kj} + \frac{\partial \mathcal{F}'_j}{\partial \phi_k} \mathcal{D}_{ki} - \mathcal{F}'_k \frac{\partial \mathcal{D}_{ij}}{\partial \phi_k}. \end{aligned} \quad (40)$$

The second-order term  $\mathcal{L}_F^{(2)}$  is given by

$$\begin{aligned} \mathcal{L}_F^{(2)}(P) &= \text{div}(\mathcal{F}_F^{(2)}P) + \text{div}_2(\mathcal{D}_F^{(2)}P), \\ \mathcal{F}_F^{(2)} &:= \sum_{m \neq 0} \left\{ \frac{\text{drf}[\text{drf}[\mathcal{F}_0, \mathcal{F}_m, \mathcal{D}], \mathcal{F}_{-m}, \mathcal{D}]}{2(m\omega)^2} \right. \\ & \quad \left. + \sum_{m' \neq 0, m} \frac{-[\mathcal{F}_{-m'}, [\mathcal{F}_{m-m'}, \mathcal{F}_m]_{\text{cl}}]_{\text{cl}}}{3mm'\omega^2} \right\}, \\ \mathcal{D}_F^{(2)} &:= \sum_{m \neq 0} \frac{\text{diff}[\mathcal{F}_{-m}, \text{diff}(\mathcal{F}_m, \mathcal{D})]}{2(m\omega)^2}, \end{aligned} \quad (41)$$

which indicates that not only the drift vector but also the diffusion matrix is renormalized at the second order. The micromotion operator  $\mathcal{G}_F^{(2)}$  is given by

$$\begin{aligned} \mathcal{G}_F^{(2)}(P) &= \text{div}(\mathcal{F}_{F,\text{mic}}^{(2)}P) + \text{div}_2(\mathcal{D}_{F,\text{mic}}^{(2)}P), \\ \mathcal{F}_{F,\text{mic}}^{(2)} &= - \sum_{m \neq 0} \left\{ \frac{\text{drf}[\mathcal{F}_0, \mathcal{F}_{-m}, \mathcal{D}] e^{im\omega t}}{(m\omega)^2} \right. \\ & \quad \left. + \sum_{m' \neq 0, m} \frac{[\mathcal{F}_{m'}, \mathcal{F}_{-m}]_{\text{cl}} e^{i(m-m')\omega t}}{2m(m-m')\omega^2} \right\}, \\ \mathcal{D}_{F,\text{mic}}^{(2)} &= - \sum_{m \neq 0} \frac{\text{diff}[\mathcal{F}_{-m}, \mathcal{D}] e^{im\omega t}}{(m\omega)^2}. \end{aligned} \quad (42)$$

In this case, the renormalized drift field  $\mathbf{f}$  and the diffusion matrix  $G$  is determined from Eq. (10).

### III. KAPITZA PENDULUM WITH FRICTION

In this section, we take the Kapitza pendulum [50] with friction as an example of a driven dissipative few-body system to test the validity of our high-frequency expansion as its effective description.

#### A. Setup

The Kapitza pendulum is a classical rigid pendulum with a vertically oscillating point of suspension (see Fig. 2), where  $\theta$  is the angle measured from the downward position,  $\omega_0 = \sqrt{g/l}$  is the frequency of the small oscillations near  $\theta = 0$  ( $g$  and  $l$  are the gravitational constant and the length of the pendulum, respectively). The suspension point oscillates with amplitude  $a$  and frequency  $\omega$ :  $y_c = -a \cos(\omega t)$ . Its EOM reads [2, 40, 50]

$$\ddot{\theta} = - \left[ \omega_0^2 + \frac{a}{l} \omega^2 \cos(\omega t) \right] \sin \theta. \quad (43)$$

While the first term on the right-hand side describes the gravitational force, the second one comes from the oscillation of the suspension point. This EOM is valid on the non-inertial frame that one oscillates together with the suspension. As is first shown by Kapitza, the highest point  $\theta = \pi$  becomes stable above the critical frequency  $\omega_c = \sqrt{2}l\omega_0/a$ , and the pendulum performs oscillations around this inverted position. From the Floquet viewpoint, the dynamics of the pendulum is described by a time-independent effective Hamiltonian, with its effective potential developing a local minimum at  $\theta = \pi$  for  $\omega > \omega_c$  [2, 40, 50]. The Kapitza pendulum is a prototypical example of dynamical stabilization, a stabilization of a system by a periodic drive, which is widely employed in many areas of physics [51–53, 105–107] including beam focusing in a synchrotron (alternating-gradient focusing [52, 53]), and trapping ions in the Paul trap [51].

We introduce a friction term  $-\gamma\dot{\theta}$  to make sure that the system reaches to a stable point after a long time. The EOM with the friction is given by

$$\ddot{\theta} = -\gamma\dot{\theta} - \left[ \omega_0^2 + \frac{a}{l} \omega^2 \cos(\omega t) \right] \sin \theta. \quad (44)$$

We note that Eq. (44) is no longer a Hamilton equation due to the friction term. In the following, we analyze this EOM using the high-frequency expansion in the previous section and confirm that it correctly reproduces the time evolution of the pendulum and the stability at the inverted point  $\theta = \pi$ .

#### B. FM expansion and effective EOM

To apply the general formalism developed in Sec. II C, we rewrite Eq.(44) into a first-order ordinary differential

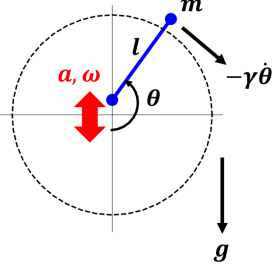


FIG. 2. Schematic illustration of the Kapitza pendulum, where  $a$  and  $\omega$  are the amplitude and frequency of the vertical oscillation of the suspension point, respectively. Here,  $\theta$ ,  $l$ , and  $g$  are the angle measured from the downward position, the length of the pendulum, and the gravitational constant, respectively.

equation of  $\theta$  and  $v$ , the angular velocity, as follows:

$$\begin{aligned}\dot{\theta} &= v \\ \dot{v} &= -\gamma v - \left[ \omega_0^2 + \frac{a}{l} \omega^2 \cos(\omega t) \right] \sin \theta.\end{aligned}\quad (45)$$

Comparing with Eq. (1), we find that the classical variable  $\phi$  in the Kapitza pendulum consists of a two-dimensional vector:  $\phi = (\theta, v)$ . The Fourier components of the drift force  $\mathbf{f}(\phi, t) := \mathbf{f}_0 + \mathbf{f}_1 e^{-i\omega t} + \mathbf{f}_{-1} e^{i\omega t}$  are given by

$$\begin{aligned}\mathbf{f}_0(v, \theta) &:= \begin{pmatrix} \mathbf{f}_{0,\theta} \\ \mathbf{f}_{0,v} \end{pmatrix} = \begin{pmatrix} v \\ -\gamma v - \omega_0^2 \sin \theta \end{pmatrix}, \\ \mathbf{f}_{\pm 1}(v, \theta) &:= \begin{pmatrix} \mathbf{f}_{\pm 1,\theta} \\ \mathbf{f}_{\pm 1,v} \end{pmatrix} = \begin{pmatrix} 0 \\ -\frac{a\omega^2}{2l} \sin \theta \end{pmatrix},\end{aligned}\quad (46)$$

and the diffusion matrix  $g$  vanishes. From the FM expansion (23), we obtain the effective drift field  $\mathbf{f}_F^{(2)}(v, \theta)$

$$\begin{aligned}[\mathbf{f}_0, \mathbf{f}_1]_{\text{cl}} &= f_{0,\theta} \frac{\partial \mathbf{f}_1}{\partial \theta} + f_{0,v} \frac{\partial \mathbf{f}_1}{\partial v} - f_{1,\theta} \frac{\partial \mathbf{f}_0}{\partial \theta} - f_{1,v} \frac{\partial \mathbf{f}_0}{\partial v} \\ &= \frac{a\omega^2}{2l} \begin{pmatrix} \sin \theta \\ -v \cos \theta - \gamma \sin \theta \end{pmatrix}, \\ \mathbf{f}_F^{(2)}(v, \theta) &:= -\frac{[\mathbf{f}_{-1}, [\mathbf{f}_0, \mathbf{f}_1]_{\text{cl}}]_{\text{cl}} + [\mathbf{f}_1, [\mathbf{f}_0, \mathbf{f}_{-1}]_{\text{cl}}]_{\text{cl}}}{2\omega^2} \\ &= \begin{pmatrix} 0 \\ -\left(\frac{a\omega}{2l}\right)^2 \sin(2\theta) \end{pmatrix},\end{aligned}\quad (47)$$

where the effective EOM is given as follows:

$$\begin{aligned}\dot{\theta} &= v \\ \dot{v} &= -\gamma v - \omega_0^2 \sin \theta - \left(\frac{a\omega}{2l}\right)^2 \sin(2\theta).\end{aligned}\quad (48)$$

Comparing Eqs. (45) and (48), we find that the original static potential  $-\omega_0^2 \cos \theta$  is replaced by the effective potential

$$V_F(\theta) = -\omega_0^2 \cos \theta - \left(\frac{a\omega}{2l}\right)^2 \sin^2 \theta \quad (49)$$

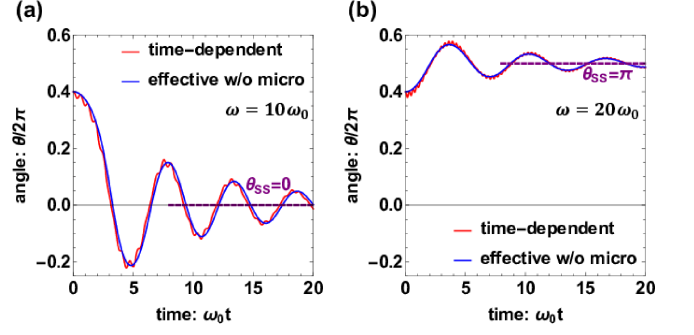


FIG. 3. Time evolution of angle  $\theta(t)$  for (a) slow ( $\omega/\omega_0 = 10$ ) and (b) fast ( $\omega/\omega_0 = 20$ ) drive, where the parameters are chosen as  $a/l = 0.1$  and  $\gamma/\omega_0 = 0.2$ . The red and blue curves are obtained by solving the time-dependent EOM (45) and the effective EOM (48), respectively, which are in nice agreements. Starting from the same initial state  $\theta_0 = 0.8\pi$  with  $v = 0$ , the angle goes to 0 for the slow drive (a), while it goes to  $\pi$  for the fast drive (b), as shown in the purple lines. The purple dashed lines show the steady-state angles  $\theta_{SS}$ , which is either 0 or  $\pi$ .

due to the periodic drive. We note that  $V_F(\theta)$  is independent of the friction strength  $\gamma$  and the same as the one obtained from the analysis without friction [40, 50]. Due to the second term, the effective potential develops a new local minimum at  $\theta = \pi$  above critical driving frequency  $\omega_c = (\sqrt{2}l\omega_0)/a$ . Since  $(\theta, v) = (0, 0)$  and  $(\pi, 0)$  are both stationary solutions of Eq. (48), the system converges to either of these points after sufficiently long time with the help of the friction  $-\gamma v$ . The steady-state angle  $\theta_{SS} := \theta(t \rightarrow \infty)$ , in general, depends on  $\theta_0$ ,  $\omega$ ,  $v(t=0)$ , and  $\gamma$ , as we will see below.

### C. Comparison between the time-periodic and effective EOMs

In what follows, we compare Eqs. (45) and (48) through the dynamics of  $\theta(t)$  and the steady-state angle  $\theta_{SS}$ . The parameters  $a/l$  and  $\gamma$  are fixed as  $a/l = 0.1$  and  $\gamma = 0.2\omega_0$ . The time evolutions of  $\theta(t)$  for low ( $\omega/\omega_0 = 10$ ) and high ( $\omega/\omega_0 = 20$ ) driving frequencies are shown in Figs. 3 (a) and (b), respectively. The initial states are taken to be the same in both cases:  $(\theta, v) = (0.8\pi, 0)$ . The red and blue curves are obtained from the time-dependent EOM (45) and the effective EOM (48), respectively, which are in good agreements. After a sufficiently long time, the pendulum approaches to the lowest point  $\theta = 0$  for the slow drive (a) below the critical frequency  $\omega_c$ , while it approaches the inverted point  $\theta = \pi$  for the fast drive (b).

In Fig. 4 (a), we present the steady-state “phase diagram” of the pendulum for fixed parameters  $v(t=0) = 0$  and  $\gamma = 0.2\omega_0$ . We see that the inverted point  $\theta = \pi$  is preferred for an initial angle close to  $\pi$  with a fast drive [shaded region in Fig. 4 (a)], while it goes to the lowest



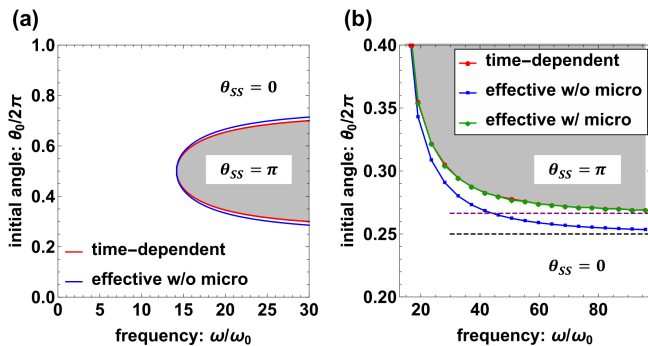


FIG. 4. (a): Dependence of the steady-state angle  $\theta_{SS}$  on the initial state  $[\theta(0), v(0)] = (\theta_0, 0)$  and frequency  $\omega$ , where  $a/l$  and  $\gamma/\omega_0$  are fixed in the same parameters as Fig. 3. In the shaded region, the angle goes to  $\theta = \pi$  after sufficiently long time, while it goes to  $\theta = 0$  in the other area. The red and blue curves show the boundary obtained from the time-dependent EOM (45) and that derived from the effective EOM (48), respectively. (b): Boundary of the steady-state angle  $\theta_{SS} = 0, \pi$  obtained from the time-dependent EOM (45) (red) and the time-independent effective EOM (48) (blue), and the time-independent effective EOM (48) in addition to the micromotion operator (green). The red and green curves are almost overlapping. The black and purple lines are guides to the eyes.

point  $\theta = 0$  for the other parameter region. The boundary curve between  $\theta_{SS} = 0$  and  $\pi$  for the effective EOM is determined from the effective potential (49) as follows:

$$\omega > \omega_c \quad \text{and} \quad |\theta - \pi| < \arccos \left[ \left( \frac{\omega_c}{\omega} \right)^2 \right]. \quad (50)$$

Although the effective EOM (48) [blue line in Fig. 4 (a)] gives a boundary (50) close to the curve obtained from the time-dependent EOM (45) [red line in Fig. 4 (a)], this slight deviation can be seen even in high frequency, which might contradicts with the validity of the high-frequency expansion. In particular, in the high-frequency limit,  $\theta_{SS}/(2\pi)$  converges to  $1/4$  for the effective EOM (dashed black line in Fig. 4 (b)), while it converges to  $0.267$  for the EOM (dashed purple line in Fig. 4 (b)). This deviation is attributed to the  $\omega$ -dependent coefficient in the drive:  $\mathbf{f}_{\pm 1} \propto \omega^2$ . Since we here fix  $a/l$  rather than the coefficient  $a\omega^2/(2l)$  of  $\mathbf{f}_{\pm 1}$ , the resulting potential, the second term on the right-hand-side of Eq. (49), is proportional to  $\omega^2$ . However, when we take into account the micromotion operator  $U_F$  in Eq. (15), we obtain an excellent agreement (almost overlapped) between the EOM and the effective EOM, shown as the red and green line in Fig. 4 (b), respectively.

#### IV. STOCHASTIC LANDAU-LIFSHITZ-GILBERT EQUATION

In this section, we treat a classical driven many-spin system described by the time-dependent sLLG equation

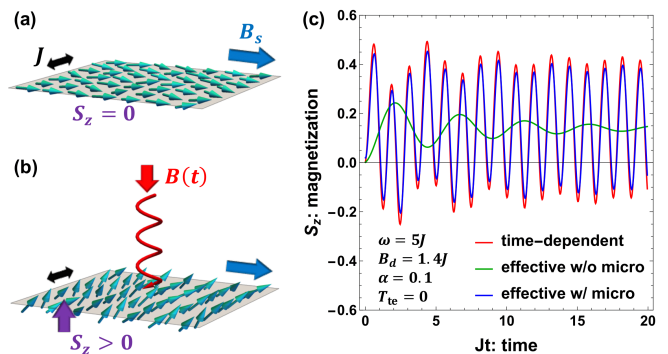


FIG. 5. (a) Schematic illustration of a two-dimensional ferromagnet with  $100 \times 100$  spins. The nearest-neighbor spins are coupled with ferromagnetic interaction with  $J$  and the static field with strength  $B_s$  is applied in the  $m_x$  direction. (b) When the system is irradiated by a circularly polarized magnetic field with strength  $B_d$ , the average magnetization  $S_z$  emerges. (c) Time evolution of the averaged magnetization  $\langle S_z \rangle$  for the original sLLG equation (53) (red), the effective sLLG (62) with (blue) and without (green) the kick operator. The parameters are chosen as  $J = 1$ ,  $\omega = 5J$ ,  $B_d = 1.4J$ ,  $B_s = 1.4J$ ,  $\alpha = 0.1$ , and  $T_{te} = 0$ .

as an example of driven many-body systems. We show that a circularly polarized electromagnetic wave generates the magnetization parallel to its propagating direction in classical ordered magnets, which is a manifestation of laser-driven Floquet engineering of magnetizations. By calculating the time-evolution of the magnetization and its expectation value at the NESS, we compare the time-dependent sLLG equation and the effective sLLG equation obtained from the FM expansion. Through a detailed comparison changing various parameters, e.g., frequency, dissipation strength, and temperature, we find that the effective one well approximates the time-dependent one for a long time up to the NESS.

In recent years, driven quantum spin systems have been studied by applying Floquet theory [4, 30–33, 94, 95]. However, it is, in general, hard to theoretically include the effects of dissipation and temperature in such driven quantum many-body systems. As we will see below, the framework based on the sLLG equation and the FM expansion enables us to treat all these effects with system size much larger than quantum cases.

#### A. Setup

The sLLG equation is a phenomenological equation of ferromagnets, which is formally the torque equation incorporated by the damping and the thermal fluctuation. It is widely used in the field of spintronics and proved to be a powerful approach to modeling ultrafast magnetization processes [1] like the laser-induced demagnetization of ferromagnets [108–110]. Let  $\mathbf{m}_r$  and  $\mathcal{H}(t)$  be the magnetic moment at site  $\mathbf{r}$  and the Hamiltonian (energy) of

the system, respectively. The sLLG equation reads

$$\dot{\mathbf{m}}_{\mathbf{r}} = -\gamma \mathbf{m}_{\mathbf{r}} \times [\mathbf{H}_{\mathbf{r}}(t) + \mathbf{h}_{\mathbf{r}}(t)] + \frac{\alpha}{m_s} \mathbf{m}_{\mathbf{r}} \times \dot{\mathbf{m}}_{\mathbf{r}}. \quad (51)$$

where  $\mathbf{H}_{\mathbf{r}}(t) = -(\delta\mathcal{H}(t))/(\delta\mathbf{m}_{\mathbf{r}})$  is the effective magnetic field generated by the surrounding spins and the external fields, and  $\mathbf{h}_{\mathbf{r}}(t)$  is the random magnetic field at  $\mathbf{r}$  modeling the thermal fluctuations. Here,  $\alpha, \gamma$ , and  $m_s := |\mathbf{m}_{\mathbf{r}}|$  are the Gilbert damping constant, the gyromagnetic ratio, and the magnitude of the magnetization, respectively. In what follows, we set  $\gamma = m_s = 1$ . The first term on the right-hand side of Eq. (51) describes the precession around  $\mathbf{H}_{\mathbf{r}}(t) + \mathbf{h}_{\mathbf{r}}(t)$ , while the second term, the so-called Gilbert term, describes damping toward the effective magnetic field. The thermal fluctuation with temperature  $T_{\text{te}}$  is modeled by  $\mathbf{h}_{\mathbf{r}}(t) := [h_{\mathbf{r},1}(t), h_{\mathbf{r},2}(t), h_{\mathbf{r},3}(t)]$  satisfying

$$\langle h_{\mathbf{r},a}(t) h_{\mathbf{r}',b}(t') \rangle = 2D \delta_{ab} \delta_{\mathbf{r},\mathbf{r}'} \delta(t-t'), \quad (52)$$

where  $D = 2k_B T_{\text{te}} \alpha$  is the diffusion constant satisfying the fluctuation-dissipation theorem. To apply the general formalism developed in Sec.II, we rewrite Eq. (51) as

$$\begin{aligned} \dot{\mathbf{m}}_{\mathbf{r}} = & -\frac{\mathbf{m}_{\mathbf{r}}}{1+\alpha^2} \times \{\mathbf{H}_{\mathbf{r}}(t) + \mathbf{h}_{\mathbf{r}}(t) \\ & + \frac{\alpha}{m_s} \mathbf{m}_{\mathbf{r}} \times [\mathbf{H}_{\mathbf{r}}(t) + \mathbf{h}_{\mathbf{r}}(t)]\}, \end{aligned} \quad (53)$$

and henceforth use this equation.

Comparing Eqs. (3) and (53), we find that  $\phi_{\mathbf{r}} = \mathbf{m}_{\mathbf{r}}$  represents the spin configuration, and  $\mathbf{f}_{\mathbf{r}}$  and  $\mathbf{g}_{\mathbf{r}}$  are given by

$$\begin{aligned} \mathbf{f}_{\mathbf{r}}(t) = & -\frac{\mathbf{m}_{\mathbf{r}}}{1+\alpha^2} \times \left[ \mathbf{H}_{\mathbf{r}}(t) + \frac{\alpha}{m_s} \mathbf{m}_{\mathbf{r}} \times \mathbf{H}_{\mathbf{r}}(t) \right] \\ & + \frac{2D}{1+\alpha^2} \mathbf{m}_{\mathbf{r}}, \\ g_{\mathbf{r},ab} = & \frac{1}{1+\alpha^2} \epsilon_{abc} m_{\mathbf{r},c} + \frac{\alpha m_s}{1+\alpha^2} \left( \delta_{ab} - \frac{m_{\mathbf{r},a} m_{\mathbf{r},b}}{(m_s)^2} \right). \end{aligned} \quad (54)$$

Here,  $\mathbf{f}_{\mathbf{r}}$  and  $\mathbf{g}_{\mathbf{r}}$  represent the spin precession generated by  $\mathbf{H}_{\mathbf{r}}$  and the spin diffusion induced by  $\mathbf{h}_{\mathbf{r}}$  and perpendicular to  $\mathbf{m}_{\mathbf{r}}$ , respectively [111, 112]. We note that the second term in  $\mathbf{f}_{\mathbf{r}}(t)$  comes from  $d_k := -D g_{kl} \partial_k g_{il}$  in Eq. (10). The probability current  $\mathbf{J}$  in the Fokker-Planck equation of the sLLG equation satisfies  $\mathbf{J} \cdot \mathbf{m} = 0$ , implying the conservation of the magnitude of the magnetic moment  $\partial_t [(\mathbf{m}_i, \mathbf{m}_i)] = 0$ .

As a simple example, we here consider a classical ferromagnetic Heisenberg model on a square lattice [see Fig. 5 (a)], whose Hamiltonian  $\mathcal{H}(t)$  reads

$$\mathcal{H}(t) = -J \sum_{\langle \mathbf{r}, \mathbf{r}' \rangle} \mathbf{m}_{\mathbf{r}} \cdot \mathbf{m}_{\mathbf{r}'} - g \mu_B \sum_{\mathbf{r}} \mathbf{B}(t) \cdot \mathbf{m}_{\mathbf{r}}, \quad (55)$$

where  $J > 0$  is the ferromagnetic coupling constant  $\mathbf{B}(t)$  is the external magnetic field we apply ( $g$  is the Lande's  $g$

factor and  $\mu_B$  is the Bohr magneton). The sum  $\sum_{\langle \mathbf{r}, \mathbf{r}' \rangle}$  is taken over all the pairs of the nearest-neighbor sites. We measure the external magnetic field in the unit of  $g \mu_B$  and thereby set  $g \mu_B = 1$ . We apply a circularly polarized driving magnetic field with strength  $B_d$  in the  $(S_x, S_y)$  plane [see Fig. 5 (b)]. The total field  $\mathbf{B}(t)$  is given by

$$\mathbf{B}(t) = (B_s + B_d \cos(\omega t), -B_d \sin(\omega t), 0)^{\text{tr}}, \quad (56)$$

which is decomposed into the Fourier harmonics as follows:

$$\begin{aligned} \mathbf{B}(t) = & \mathbf{B}_0 + \mathbf{B}_1 e^{-i\omega t} + \mathbf{B}_{-1} e^{i\omega t}, \\ \mathbf{B}_0 = & (B_s, 0, 0)^{\text{tr}}, \\ \mathbf{B}_{\pm 1} = & \frac{B_d}{2} (1, \mp i, 0)^{\text{tr}}. \end{aligned} \quad (57)$$

For real magnetic materials, the typical value of the exchange interaction  $J$  is the order of 1–10 meV. Therefore, the frequency  $\omega$  of applied electromagnetic waves should be the same as the energy scale of  $J$ , corresponding to the range from gigahertz to terahertz. The model (55) would be relevant for the laser-driven spin dynamics in ordered magnets. The quantum analog of the model (55) with an anisotropic term has been studied in Refs. [30, 31].

## B. FM expansion and the effective sLLG

Then, the Fourier harmonics  $\mathbf{f}_{\pm 1}$  and the resultant first-order FM drift force  $\mathbf{f}_{F,\mathbf{r}}^{(1)}$  are given from Eqs.(30) and (54) as follows (see App. A for the derivation):

$$\begin{aligned} \mathbf{f}_{\pm 1, \mathbf{r}} = & -\frac{\mathbf{m}_{\mathbf{r}}}{1+\alpha^2} \times \left( \mathbf{B}_{\pm 1} + \frac{\alpha}{m_s} \mathbf{m}_{\mathbf{r}} \times \mathbf{B}_{\pm 1} \right), \\ \mathbf{f}_{F,\mathbf{r}}^{(1)} = & \frac{i}{\omega} \left[ \mathbf{f}_{1,\mathbf{r}} \cdot \frac{\delta \mathbf{f}_{-1,\mathbf{r}}}{\delta \mathbf{m}_{\mathbf{r}}} - \mathbf{f}_{-1,\mathbf{r}} \cdot \frac{\delta \mathbf{f}_{1,\mathbf{r}}}{\delta \mathbf{m}_{\mathbf{r}}} \right] \\ = & -\frac{\mathbf{m}_{\mathbf{r}}}{1+\alpha^2} \times \left( \mathbf{H}_{F,\mathbf{r}}^{(1)} + \frac{\alpha}{m_s} \mathbf{m}_{\mathbf{r}} \times \mathbf{H}_{F,\mathbf{r}}^{(1)} \right), \\ \mathbf{H}_{F,\mathbf{r}}^{(1)} = & \frac{i \mathbf{B}_{-1} \times \mathbf{B}_{+1}}{(1+\alpha^2)\omega} - \alpha \frac{i \mathbf{B}_{-1} \times \mathbf{B}_{+1}}{(1+\alpha^2)\omega} \times \mathbf{m}_{\mathbf{r}}. \end{aligned} \quad (58)$$

While the first term in  $\mathbf{H}_{F,\mathbf{r}}^{(1)}$  describes the effective magnetic field with

$$\mathbf{b}^{(1)} := \frac{i \mathbf{B}_{-1} \times \mathbf{B}_{+1}}{(1+\alpha^2)\omega} = \frac{(B_d)^2}{2\omega(1+\alpha^2)} \hat{z}, \quad (59)$$

the second term describes the so-called spin-transfer torque [113–116]. The effective field parallel to  $i(\mathbf{B}_{-1} \times \mathbf{B}_{+1})$  is the dominant term of the FM expansion, and thereby we can predict that the circularly polarized laser changes the value of the magnetization along  $i(\mathbf{B}_{-1} \times \mathbf{B}_{+1})$ . The emergence of this effective magnetic field can be qualitatively understood from an analog with a quantum system: in the presence of the external drive

$\hat{H}(t) = -\mathbf{B}(t) \cdot \hat{\mathbf{S}}$ , with  $\hat{\mathbf{S}}$  being the total spin operator in the quantum system, the first-order FM Hamiltonian

$$\hat{H}_F^{(1)} := \frac{[\hat{H}_{-1}, \hat{H}_1]}{\omega} = \frac{i}{\omega} (\mathbf{B}_{-1} \times \mathbf{B}_{+1}) \cdot \hat{\mathbf{S}} \quad (60)$$

represents the effective magnetic field  $i(\mathbf{B}_{-1} \times \mathbf{B}_{+1})/\omega$  [30, 31]. However, we find from Eqs. (58) that its magnitude decreases with factor  $(1 + \alpha^2)^{-1}$ . Moreover, there appears the spin-transfer torque as a consequence of the coupling with the environment, while it always vanishes in a closed spin system. The drift field  $\tilde{\mathbf{f}}_{\text{mic},\mathbf{r}}^{(1)}$  corresponding to the kick operator  $\mathcal{G}_F^{(1)}$  in Eq. (32) is given by

$$\tilde{\mathbf{f}}_{\text{mic},\mathbf{r}}^{(1)}(\mathbf{m}_{\mathbf{r}}, t) := -\frac{\mathbf{m}_{\mathbf{r}}}{1 + \alpha^2} \times \left( \mathbf{H}_{\text{mic}}^{(1)}(t) + \frac{\alpha}{m_s} \mathbf{m}_{\mathbf{r}} \times \mathbf{H}_{\text{mic}}^{(1)}(t) \right), \quad (61)$$

where  $\mathbf{H}_{\text{mic}}^{(1)}(t) = i(\mathbf{B}_{-1}e^{i\omega t} - \mathbf{B}_{+1}e^{-i\omega t})$  describes an oscillating magnetic field.

The second-order expansion term is much more complicated due to the renormalization of the diffusion matrix  $G$ . The obtained sLLG equation is given as follows (see App. A for the derivation):

$$\dot{\mathbf{m}}_{\mathbf{r}} = -\frac{\mathbf{m}_{\mathbf{r}}}{1 + \alpha^2} \times \left[ \mathbf{H}_{F,\mathbf{r}} + \sqrt{1 + \chi_{\mathbf{r}}} \mathbf{h}_{\mathbf{r}} \right] + \frac{\alpha}{m_s} \mathbf{m}_{\mathbf{r}} \times \left( \mathbf{H}_{F,\mathbf{r}} + \sqrt{1 + \chi_{\mathbf{r}}} \mathbf{h}_{\mathbf{r}} \right). \quad (62)$$

The effective magnetic field  $\mathbf{H}_{F,\mathbf{r}}$  and the correction to the diffusion term  $\chi_{\mathbf{r}}(\mathbf{m}_{\mathbf{r}})$  are given by

$$\mathbf{H}_{F,\mathbf{r}} := \sum_{\mathbf{r}':\text{n.n.}} (J\mathbf{m}_{\mathbf{r}'} + \delta\mathbf{J}_{\mathbf{r},\mathbf{r}'}) + \mathbf{B}_F + \mathbf{V}_F \times \mathbf{m}_{\mathbf{r}},$$

$$\chi_{\mathbf{r}}(\mathbf{m}_{\mathbf{r}}) := -\left( \frac{\alpha B_d}{m_s \omega (1 + \alpha^2)} \right)^2 \frac{3(m_s)^2 - (m_{\mathbf{r},z})^2}{2}, \quad (63)$$

where the sum  $\sum_{\mathbf{r}':\text{n.n.}}$  is taken over the nearest-neighbor sites of  $\mathbf{r}$ . The total effective external magnetic field  $\mathbf{B}_F$ , the spin-transfer torque  $\mathbf{V}_F$ , and the effective interaction are given by

$$\mathbf{B}_F := \mathbf{B}_0 + \mathbf{b}^{(1)} + (1 - \alpha^2)\mathbf{b}^{(2)} - \frac{\alpha m_s D}{2(1 + \alpha^2)} \frac{\delta\chi_{\mathbf{r}}}{\delta\mathbf{m}_{\mathbf{r}}},$$

$$\mathbf{V}_F := -\frac{\alpha}{m_s} \mathbf{b}^{(1)} - \frac{2\alpha}{m_s} \mathbf{b}^{(2)} + \frac{D}{2(1 + \alpha^2)} \frac{\delta\chi_{\mathbf{r}}}{\delta\mathbf{m}_{\mathbf{r}}},$$

$$\delta\mathbf{J}_{\mathbf{r},\mathbf{r}'} := J \left( \frac{\alpha B_d}{m_s \omega (1 + \alpha^2)} \right)^2 \times \sum_{\mathbf{r}':\text{n.n.}} m_{\mathbf{r}',z} \begin{pmatrix} m_{\mathbf{r}',x} \delta m_{\mathbf{r},\mathbf{r}',z} \\ m_{\mathbf{r}',y} \delta m_{\mathbf{r},\mathbf{r}',z} \\ -m_{\mathbf{r}',z} \delta m_{\mathbf{r},\mathbf{r}',x} - m_{\mathbf{r}',y} \delta m_{\mathbf{r},\mathbf{r}',y} \end{pmatrix}, \quad (64)$$

where  $\delta\mathbf{m}_{\mathbf{r},\mathbf{r}'} := \mathbf{m}_{\mathbf{r}} - \mathbf{m}_{\mathbf{r}'}$  and  $\mathbf{b}^{(2)}$  is defined by

$$\mathbf{b}^{(2)} := -\left( \frac{B_d}{2\omega(1 + \alpha^2)} \right)^2 B_s \hat{x}. \quad (65)$$

### C. Short-time dynamics

In Fig. 5 (c), we calculate the time evolution of the spatially averaged magnetization  $S_z := (1/N) \sum_{\mathbf{r}} m_{\mathbf{r},z}$ , with  $N = 100 \times 100$  being the number of spins, using three different equations: (i) the original sLLG equation (53) with driving field (red), (ii) the effective sLLG without the kick operator  $\mathcal{G}_F$  (blue), and (iii) the effective sLLG with the kick operator  $\mathcal{G}_F$  (green). We use the Heun method for numerical integration of the sLLG equation with the linearization technique [117]. The time evolution without the kick operator is obtained merely solving Eq. (62). To incorporate the kick operator, we also have to apply the operator  $\exp[-\mathcal{G}_F(0)]$  and  $\exp[\mathcal{G}_F(t)]$  to the initial state and the state at time  $t$ , respectively.

The initial state is taken as the fully polarized state:  $\mathbf{m}_{\mathbf{r}} = (1, 0, 0)^{\text{tr}}$  for all the cases. The parameters are chosen as  $J = 1, B_d = 1.4J, \omega = 5J, B_s = 1.4J, \alpha = 0.1$ , and  $T_{\text{te}} = 0$ . After a long time  $t \gg (\alpha J)^{-1}$ , the system goes to the NESS, where the magnetization oscillate around a constant value with period  $T$ . Due to the effective magnetic field  $\mathbf{b}_F^{(1)}(\parallel \hat{z})$ , the average magnetization  $S_z$  increases from 0. As we can see from Fig. 5 (c), the effective sLLG equation with the kick operator (blue) shows good agreement with the time-dependent sLLG (red). Although the effective sLLG equation without the kick operator (green) fails to capture the oscillating behavior, it well reproduces the long-time average  $\bar{S}_z$  at the steady state.

### D. NESS

In Fig. 6, we show the comprehensive analysis of the dependence of the long-time average of the magnetization  $\bar{S}_z$  on (a) driving frequency  $\omega$ , (b) driving amplitude  $B_d$ , (c) Gilbert damping  $\alpha$ , and (d) temperature  $T_{\text{te}}$ . The curves with the three colors, red, green, and blue are obtained from the three equations (i), (ii), and (iii) explained above. Except for the parameter changed in each panel, the parameters are fixed as  $J = 1, \omega = 7J, B_d = J, B_s = 1.4J, \alpha = 0.1$ , and  $T_{\text{te}} = 0.2J$ . As shown in Fig. 6 (a), the average magnetization  $\bar{S}_z(\propto \omega^{-1})$  is induced by the effective magnetic field  $\mathbf{b}^{(1)}(\propto \omega^{-1})$ , and the time-dependent sLLG (53) and the effective one (62) show excellent agreement in the high-frequency regime  $\omega/J > 5$ . In Fig. 6 (b), the driving amplitude is varied from weakly driven ( $B_d \ll J$ ) to strongly driven ( $B_d \simeq J$ ) regimes, where the effective sLLG with kick operator shows better agreement for a strong drive. The effect of dissipation is analyzed in Fig. 6 (c), where the calculation is performed from the weakly dissipative ( $\alpha \ll 1$ ) to strongly dissipative ( $\alpha \simeq 1$ ) regimes. In Fig. 6 (d), where we vary the temperature to simulate the sLLG with ( $T_{\text{te}} = 0$ ) and without ( $T_{\text{te}} > 0$ ) random field  $\mathbf{h}_{\mathbf{r}}$ . Although a slight deviation is visible between the time-dependent and effective sLLG (see the inset), the latter correctly well reproduces the temperature dependence, i.e., the slope of

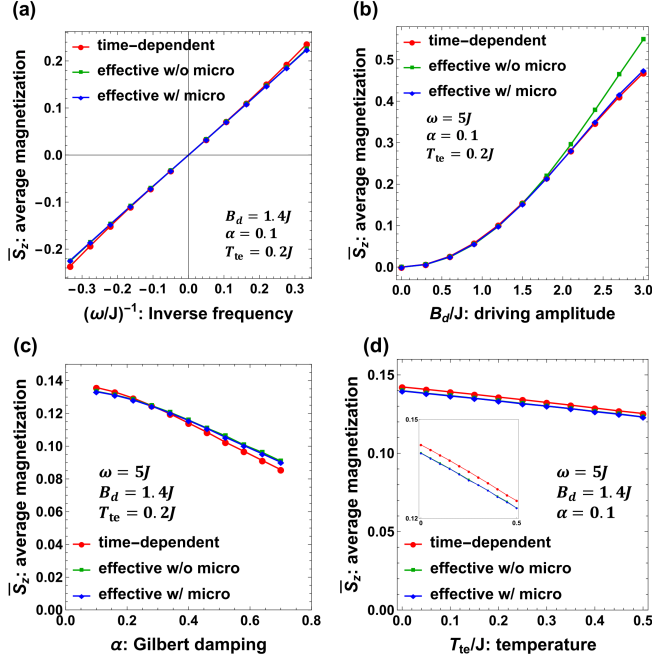


FIG. 6. Dependence of the long-time average of the magnetization  $\bar{S}_z$  on (a) driving frequency  $\omega$ , (b) driving strength  $B_d$ , (c) Gilbert damping  $\alpha$ , and (d) temperature  $T_{te}$  in the system (55). The red, green, and blue points are obtained from the time-dependent sLLG equation (53), the effective sLLG equation (62) without the kick operator, and the equation (62) with the kick operator, respectively. The parameters are fixed as  $J = 1$ ,  $\omega = 5J$ ,  $B_d = 1.4J$ ,  $B_s = 1.4J$ ,  $\alpha = 0.1$ , and  $T_{te} = 0.2J$ , except for the parameter varied in each panel. The magnetization is normalized as  $m_s = 1$ . The inset in the panel (d) shows the enlarged image between  $0.12 \leq \bar{S}_z \leq 0.15$ .

the curve. From the above results, we can conclude the effective sLLG equation obtained from the FM expansion well approximates the original one in a wide range of parameters from weak to strong dissipation and with and without a random field.

### E. Discussion

Let  $U(T, 0)$  and  $\exp(\mathcal{L}_F T)$  be the time evolution within one period generated by the time-dependent Fokker-Planck operator  $\mathcal{L}_t$  and that by its truncated FM expansion  $\mathcal{L}_F$ . The above agreement on the dynamics up to the NESS implies their difference  $\epsilon := \|U(T, 0) - \exp(\mathcal{L}_F T)\|$  is small. This indicates that the FM expansion is at least an asymptotic series, which is explained as follows. Let us write the spectrum decompositions of  $U(T, 0)$  and  $\exp(\mathcal{L}_F T)$  as

$$U(T, 0) = \sum_{\alpha} e^{-\Gamma_{\alpha} T} |v_{R,\alpha}\rangle \langle v_{L,\alpha}|, \\ \exp(\mathcal{L}_F T) = \sum_{\alpha} e^{-\Gamma_{F,\alpha} T} |v_{F,R,\alpha}\rangle \langle v_{F,L,\alpha}|, \quad (66)$$

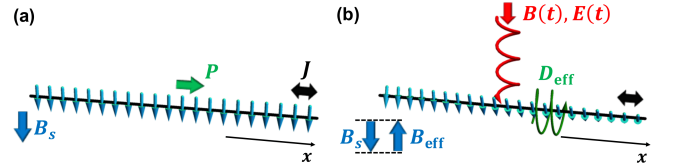


FIG. 7. (a) Schematic illustration of a multiferroic spin chain. The nearest-neighbor spins are coupled with a ferromagnetic coupling with  $J$  and the ME coupling with polarization  $P$  given by Eq. (68), and the static field  $B_s$  is applied in the  $m_z$  direction. (b) By the irradiation of the laser with electromagnetic fields,  $E(t)$  and  $B(t)$ , the effective DM interaction  $D_F$  and the effective magnetic field  $D_F$  is induced, leading to a spiral spin texture and an emergence of the vector chirality  $\mathcal{V}_x^{tot}$  along the  $x$  direction. The static field is chosen to cancel with the effective field  $B_F$ .

where  $0 = \text{Re}\Gamma_0 < \text{Re}\Gamma_1 < \text{Re}\Gamma_2$  and  $0 = \text{Re}\Gamma_{F,0} < \text{Re}\Gamma_{F,1} < \text{Re}\Gamma_{F,2}$ . The two decomposition satisfy  $\Gamma_{\alpha} \simeq \Gamma_{F,\alpha}$ ,  $|v_{R,\alpha}\rangle \simeq |v_{F,R,\alpha}\rangle$ , and  $\langle v_{L,\alpha}| \simeq \langle v_{F,L,\alpha}|$  provided that  $\epsilon$  is small. In particular, at time  $t = mT \gg t_d$ , with  $t_d$  being the typical relaxation time, the system goes to the NESS  $|v_{R,\alpha}\rangle$ , which is well approximated by  $|v_{F,R,\alpha}\rangle$ , implying that the true NESS is well approximated by that obtained from the FM expansion. Although it is unclear where the FM expansion becomes absolutely convergent even in the presence of dissipation, it is sufficient for describing the NESS provided that it asymptotically convergent. It is worth mentioning that the FM expansion is performed recently for open quantum systems and its truncation well describes the NESS [118–121], indicating that it is at least an asymptotically convergent.

## V. APPLICATION TO SPINTRONICS

Laser control of magnetic materials attracts considerable interest in recent years since it could offer an ultrafast and non-contact manipulation of magnets [1]. As demonstrated in Refs. [30–33, 94, 95], lasers can serve as a versatile tool for a dynamical control of magnets and even their intrinsic magnetic interactions, e.g., exchange interaction and Dzyaloshinskii-Moriya (DM) interaction. Multiferroics are materials that exhibit both ferromagnetism and ferroelectricity [122, 123]. Due to the coupling between the spin degrees of freedom and the electric polarization, multiferroic materials have a potentially high impact for future spintronics [73].

In this section, we consider a multiferroic spin system described by the sLLG equation. Our setup is a classical analog of Ref. [32], where a periodically driven multiferroic *quantum* spin chain was studied. While the vector spin chirality and spin current were shown to emerge in the previous study, they vanish after a long time due to the heating. On the other hand, in our setup, the system reaches the NESS with a finite vector chirality due to the balance among the driving, the heating, and the Gilbert

damping.

### A. Synthetic DM interaction in a multiferroic spin chain

The Hamiltonian  $\mathcal{H}_{\text{MF}}(t)$  is given from  $\mathcal{H}(t)$  in Eq. (55) by adding ME coupling:

$$\mathcal{H}_{\text{MF}}(t) = \mathcal{H}(t) - \mathbf{P} \cdot \mathbf{E}(t), \quad (67)$$

where the second term represent the magnetoelectric (ME) coupling of the total polarization  $\mathbf{P}$  with the external electric field  $\mathbf{E}(t)$ . We assume the antisymmetric magnetostriction mechanism (also known as the inverse DM effect mechanism [124–127]) of multiferroics:

$$\mathbf{P} = \sum_{\langle \mathbf{r}, \mathbf{r}' \rangle} \mathbf{P}_{\mathbf{r}, \mathbf{r}'} = g_{me} \sum_{\langle \mathbf{r}, \mathbf{r}' \rangle} \mathbf{e}_{\mathbf{r}, \mathbf{r}'} \times (\mathbf{m}_{\mathbf{r}} \times \mathbf{m}_{\mathbf{r}'}), \quad (68)$$

where  $\mathbf{e}_{\mathbf{r}, \mathbf{r}'} := (\mathbf{r}' - \mathbf{r})/|\mathbf{r}' - \mathbf{r}|$  is the unit vector connecting the nearest neighbor sites  $\mathbf{r}$  and  $\mathbf{r}'$ , and  $g_{me}$  denotes the magnitude of the ME coupling. This ME coupling is known to be responsible for electric polarization in a wide class of spiral ordered (i.e., chirality ordered) multiferroic magnets. Combining Eqs. (68) and (55), we obtain the explicit forms of  $\mathcal{H}_{\text{MF}}(t)$  and the effective field  $\mathbf{H}_{\mathbf{r}}(t)$ :

$$\begin{aligned} \mathcal{H}_{\text{MF}}(t) &= - \sum_{\langle \mathbf{r}, \mathbf{r}' \rangle} [J\mathbf{m}_{\mathbf{r}} \cdot \mathbf{m}_{\mathbf{r}'} + \mathbf{D}_{\mathbf{r}, \mathbf{r}'}(t) \cdot (\mathbf{m}_{\mathbf{r}} \times \mathbf{m}_{\mathbf{r}'})] \\ &\quad - \sum_{\mathbf{r}} [\mathbf{B}_s + \mathbf{B}(t)] \cdot \mathbf{m}_{\mathbf{r}}, \\ \mathbf{H}_{\mathbf{r}}(t) &= \sum_{\mathbf{r}': n.n.} (J\mathbf{m}_{\mathbf{r}'} + \mathbf{D}_{\mathbf{r}, \mathbf{r}'}(t) \times \mathbf{m}_{\mathbf{r}'} + \mathbf{B}_s + \mathbf{B}(t), \end{aligned} \quad (69)$$

where  $\mathbf{D}_{\mathbf{r}, \mathbf{r}'}(t) := g_{me}\mathbf{E}(t) \times \mathbf{e}_{\mathbf{r}, \mathbf{r}'}$  is the DM coupling induced by the electric field. To demonstrate the emergence of a spin texture by a laser, we here a spin chain aligned along the  $x$  direction irradiated by the laser field traveling along the ( $-z$ ) direction (see Fig. 7 (a)). Although a realistic multiferroic system has a strong three-dimensional nature [128, 129], we here consider a one-dimensional chain for simplicity. The electric field  $\mathbf{E}(t)$  and magnetic field  $\mathbf{B}(t)$  of an applied circularly-polarized electromagnetic wave are given by

$$\begin{aligned} \mathbf{E}(t) &= E_0 (\sin(\omega t), \cos(\omega t), 0)^{\text{tr}}, \\ \mathbf{B}(t) &= \frac{-\hat{z}}{c} \times \mathbf{E} = \frac{E_0}{c} (\cos(\omega t), -\sin(\omega t), 0)^{\text{tr}}. \end{aligned} \quad (70)$$

From the first-order FM expansion, the effective static

field  $\mathbf{H}_{\mathbf{r}, F}$  at site  $\mathbf{r}$  is given from Eq. (30) by

$$\begin{aligned} \mathbf{H}_{\mathbf{r}, F} &:= \sum_{\mathbf{r}': n.n.} [J\mathbf{m}_{\mathbf{r}'} + \mathbf{D}_{F, \mathbf{r}, \mathbf{r}'} \times \mathbf{m}_{\mathbf{r}'}] + \mathbf{B}_s + \mathbf{B}_F \\ &\quad - \alpha \mathbf{B}_F \times \mathbf{m}_{\mathbf{r}} \\ &\quad - \sum_{\mathbf{r}': n.n.} \frac{\alpha \epsilon_E \epsilon_B}{2m_s(1 + \alpha^2)\omega} \begin{pmatrix} m_s^2 + m_{\mathbf{r}', y} \delta m_{\mathbf{r}, y} \\ -m_{\mathbf{r}', y} \delta m_{\mathbf{r}, x} \\ 0 \end{pmatrix}, \\ \mathbf{D}_{F, \mathbf{r}, \mathbf{r}'} &= \frac{\epsilon_E \epsilon_B}{2(1 + \alpha^2)\omega} \mathbf{e}_{\mathbf{r}, \mathbf{r}'} =: D_F \mathbf{e}_{\mathbf{r}, \mathbf{r}'}, \\ \mathbf{B}_F &= \frac{\epsilon_B^2}{2(1 + \alpha^2)\omega} \hat{z}, \end{aligned} \quad (71)$$

where  $\epsilon_E := g_{me}E_0$  and  $\epsilon_B := (g\mu_B E_0)/c$  are the normalized electric and magnetic energies, respectively (see App. A for the derivation). The strongest magnetic field  $\epsilon_B$  of terahertz (THz) lasers attains 1 - 10 T [130, 131] and the magnitude of  $g_{me}$  can be large in a gigahertz (GHz) to THz region [125, 132–134]. For standard magnets with  $J = 0.1 - 10$  meV, both  $\epsilon_E/J$  and  $\epsilon_B/J$  can achieve values of 0.1 - 1. Second and third terms in  $\mathbf{H}_{F, \mathbf{r}}$  are the laser-driven DM interaction generated via the single-photon absorption and emission, and the synthetic magnetic field appeared in Sec. IV. Equation (71) shows that a synthetic DM field  $\mathbf{D}_{F, \mathbf{r}, \mathbf{r}'}$  emerges from along the chain the combination of the ME and Zeeman coupling.

We can ignore the second and third lines of  $\mathbf{H}_{\mathbf{r}, F}$  in Eq. (71) provided that the dissipation is weak enough  $\alpha \ll 1$ , where the resulting sLLG equation is equivalent to the sLLG equation with the static Hamiltonian

$$\mathcal{H}_F = - \sum_{j=1}^L [J\mathbf{m}_j \cdot \mathbf{m}_{j+1} + D_F \mathcal{V}_{j,x} + (\mathbf{B}_F + \mathbf{B}_s) \cdot \mathbf{m}_j], \quad (72)$$

where  $\mathcal{V}_{j,x} := \hat{x} \cdot (\mathbf{m}_j \times \mathbf{m}_{j+1})$  is the vector chirality along the  $x$  axis. One can see from Eq. (72) that the system exhibits a spiral spin texture due to the synthetic DM interaction, leading to the emergence of the vector chirality (see Fig. 7). To maximize the total vector chirality  $\mathcal{V}_x^{\text{tot}} := \sum_j \mathcal{V}_{j,x}$ , we introduce a static field  $\mathbf{B}_s$  along the  $z$  axis to cancel out with  $\mathbf{B}_F$ , i.e.,  $\mathbf{B}_s + \mathbf{B}_F = 0$ . With purely ferromagnetic and DM interactions in Eq. (72), a spin spiral state is predicted to emerge [135, 136], whose vector chirality per site is given as follows:

$$\begin{aligned} \frac{\mathcal{V}_x^{\text{tot}}}{L} &:= \frac{1}{L} \sum_j \mathcal{V}_{j,x} = \tan^{-1} \left( \frac{D_F}{J} \right) \\ &= \tan^{-1} \left[ \frac{\epsilon_E \epsilon_B}{2(1 + \alpha^2)\omega J} \right]. \end{aligned} \quad (73)$$

### B. Emergent vector chirality by laser irradiation

To demonstrate the emergent vector chirality  $\mathcal{V}_x^{\text{tot}}$  predicted from the effective theory (73), we perform a numerical simulation of the time-dependent sLLG equation

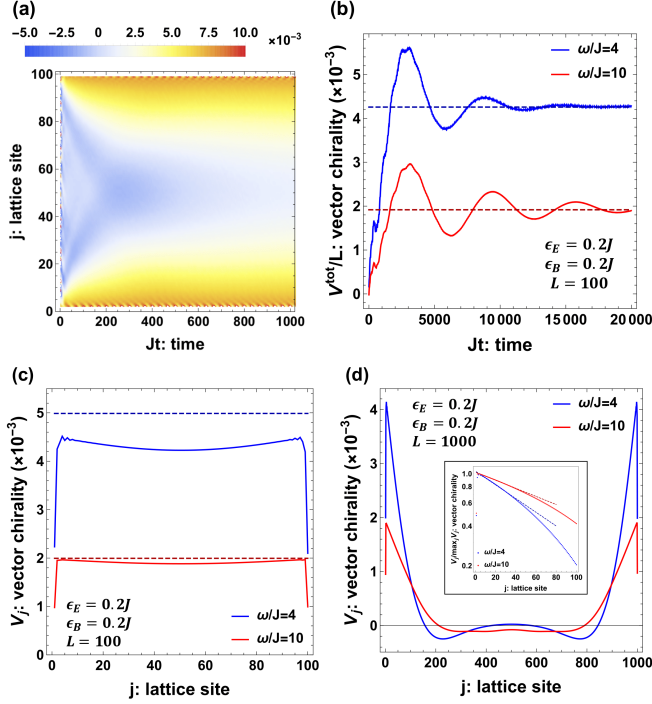


FIG. 8. (a): Spatiotemporal dynamics of the vector chirality  $[\hat{x} \cdot (\mathbf{m}_j \times (\mathbf{m}_{j+1} - \mathbf{m}_{j-1}))]/2$  with driving frequency  $\omega/J = 4$ . As time passes, the vector chirality penetrates into the system from the edges  $j = 0, L$ , where it spreads uniformly over the system after a sufficiently long time. (b): Time evolution of the spatially averaged vector chirality  $\mathcal{V}_x^{\text{tot}}/L$  with different driving frequencies  $\omega/J = 4$  (blue) and  $\omega/J = 10$  (red). The dashed lines show the values at the NESSs. (c), (d): Spatial profile of  $\mathcal{V}_{j,x}$  at NESS for two system size [ $L = 100$  for (c) and  $L = 1000$  for (d)] in the NESSs. The inset in Fig. (d) shows the logarithmic plot of  $\mathcal{V}_{j,x}/(\max_j \mathcal{V}_{j,x})$  for the first 100 sites  $0 \leq j \leq 100$ . The red and blue points and curves corresponds to the smaller ( $\omega = 4J$ ) and larger ( $\omega = 10J$ ) driving frequency.

(51) with time-dependent effective magnetic field  $\mathbf{H}_r(t)$  (69). We fix the Zeeman coupling  $\epsilon_B$ , the Gilbert damping, and temperature  $T_{\text{te}}$  as  $\epsilon_B/J = 0.2$ ,  $\alpha = 0.05$ , and  $T_{\text{te}} = 0$ , respectively. The initial state is set to be the polarized state  $\mathbf{m}_r = -\hat{z}$ , and the laser is turned on at  $t = 0$ . Since  $\mathcal{V}_{j,x}$  emerges from the edges as we will see below, we solve the LLG equation with the open boundary condition, i.e.,  $\mathbf{m}_0 = \mathbf{m}_{L+1} = \mathbf{0}$ . In Fig. 8 (a) shows the spatiotemporal dynamics of the vector chirality  $[\hat{x} \cdot (\mathbf{m}_j \times (\mathbf{m}_{j+1} - \mathbf{m}_{j-1}))]/2$ , while the time evolution of the spatially averaged vector chirality  $\mathcal{V}_x^{\text{tot}}/L$  is plotted in Fig. 8 (b). As we can see from Fig. 8 (a), the vector chirality penetrates into the system from the edges ( $j = 0, L$ ) and spreads uniformly over the system after a sufficiently long time ( $t \sim 10^4 J^{-1}$ ). Due to the balance between the drive and damping, the system reaches the NESS with constant  $\mathcal{V}_x^{\text{tot}}/L$  [dashed lines in Fig. 8 (b)]. In Fig. 8 (c) and (d), we plot the spatial profiles of  $\mathcal{V}_{j,x}$  at the NESSs for the chain lengths  $L = 100$  and  $L = 1000$ , respec-

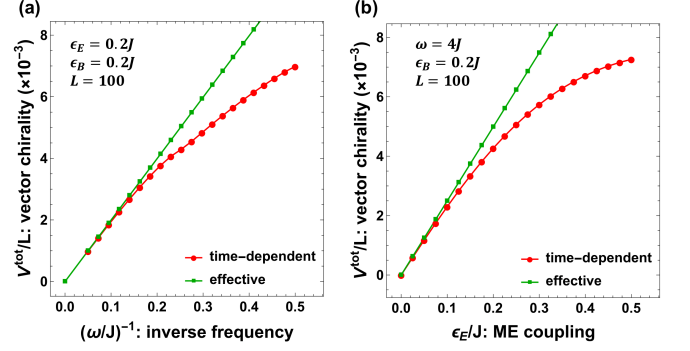


FIG. 9. (a) Dependence of the mean vector chirality  $\mathcal{V}_x^{\text{tot}}/L$  on the driving frequency  $\omega$  in the NESS with a fixed ME coupling  $\epsilon_E = 0.2J$ . (b) Dependence of the mean vector chirality  $\mathcal{V}_x^{\text{tot}}/L$  on the ME coupling  $\epsilon_E$  in the NESS with a fixed driving frequency  $\omega = 4J$ . The red curves are obtained by solving the sLLG equation with the time-dependent effective field (69) while green ones are drawn from Eq.(73), that is derived from the FM expansion (73).

tively. The vector chirality in the NESSs is localized at the edges as shown in Fig. 8 (d). However, the vector chirality uniformly spreads over the system for a smaller system ( $L = 100$ ) shown in Fig. 8 (c) due to a rather long localization length, e.g.,  $\sim 100$  sites for  $\omega/J = 4$ . Note that the localization length becomes larger for larger  $\omega$  as shown in the inset in Fig. 8 (d). This implies that one can optically induce a tunable vector chirality for nanomagnets and disordered spin systems where impurities effectively play the role of boundaries.

We finally check the validity of our effective theory quantitatively by calculating the dependence of the mean vector chirality  $\mathcal{V}_x^{\text{tot}}/L$  at the NESS on the frequency  $\omega$  and the ME coupling  $\epsilon_E$  to compare with the effective-theory result (73) quantitatively. As shown in Fig. 9, we have an excellent agreement between the original time-dependent problem with the effective-theory analysis (73) in high-frequency or weak ME-coupling regions, where the synthetic DM interaction  $D_F$  is small and hence the FM expansion is expected to be good.

## VI. CONCLUSION AND OUTLOOK

In this paper, we develop a systematic high-frequency expansion of periodically driven classical EOMs. Our formalism is applicable not only to purely classical systems but also quantum systems and to both closed and open systems at zero and finite temperatures, as far as they are described by nonlinear (stochastic) ordinary differential equations. The key idea is using the master equation corresponding to the EOM, rather than EOM itself, to apply the Floquet theorem to it (see Fig. 1). The FM expansion of the EOM is obtained from the FM expansion of the time-periodic master equation. Our method is demonstrated in a single particle system and a many-

body system, by examples of a Kapitza pendulum with friction (Sec. III) and laser-driven magnets described by the sLLG equation (Sec. IV), respectively. In both cases, the effective EOMs obtained from the FM expansion are found to be well approximate the time-dependent EOMs not only in short times but also up to their NESS. This result is in stark contrast to closed systems where the truncated FM expansion fails to capture the infinite-temperature state after the Floquet prethermalization. Finally, in Sec. V, we present an application to spintronics, demonstrating an optical generation of a spin vector chirality in a multiferroic spin chain by a circularly polarized laser.

This work opens many avenues for future exploration. First, it will be interesting to study an application to ultrafast spintronics [1]. While the Floquet engineering of magnets is mostly discussed in closed systems [30–33, 94, 95], coupling with an environment is unavoidable in any solid-state system. Also, the numerical simulation of interacting spin systems is restricted to a small system due to the exponentially increasing dimension of the Hilbert spaces, suffering from a finite-size effect. Our approach allows us to simulate driven classical spin systems with larger system sizes than quantum ones, yet to take into account the effect of dissipation and temperature at the same time. Second, the master equation offers a natural realization of a non-Hermitian Schrödinger equation [88] as mentioned in Sec. II. Recently considerable efforts have been devoted to exploring non-Hermitian physics both experimentally and theoretically [137–150], in particular, their topological aspects. Remarkably, topological classification of static non-Hermitian systems [151, 152] is found to be significantly different from the Hermitian counterpart [153–155]. Since Hermitian Floquet systems exhibit unique topological phenomena which have no counterpart to static ones, e.g., anomalous edges [24, 156, 157], it is natural to expect that non-Hermitian Floquet systems also host unique topological phases, different from both Hermitian Floquet systems and non-Hermitian static systems.

## VII. ACKNOWLEDGEMENT

We acknowledge Zongping Gong, Kazuya Fujimoto, Ryusuke Hamazaki, Fumihiro Ishikawa, Tatsuhiko N. Ikeda, Takashi Mori, Tatsuhiko Shirai, Masaru Hongo, Sota Kitamura, Takashi Oka, Alexander Schnell, and Andr Eckardt for fruitful discussions. S. H and H. F. are supported by Advanced Leading Graduate Course for Photon Science (ALPS) of Japan Society for the Promotion of Science (JSPS). S.H is supported by JSPS KAKENHI Grant-in-Aid for JSPS Fellows Grant No. JP16J03619. H.F is supported by JSPS KAKENHI Grant-in-Aid for JSPS Fellows Grant No. JP16J04752. M. S. was supported by Grant-in-Aid for Scientific Research on Innovative Area, Nano Spin Conversion Science

(Grant No.17H05174), and JSPS KAKENHI (Grant No. JP17K05513 and No. JP15H02117). A part of the computation in this work has been done using the facilities of the Supercomputer Center, the Institute for Solid State Physics, the University of Tokyo.

## Appendix A: FM expansion of the sLLG equation

In this Appendix, we explain how to compute the low-order terms of the FM expansion for the sLLG equations describing laser-driven magnets in Secs. IV and V.

### 1. Two-dimensional ferromagnet: first order

We first consider the first-order term of the FM expansion for the sLLG equation in Sec. IV. For a systematic calculation of commutators in the FM expansion, we rewrite the Fokker-Planck operator in terms of the angular momentum operators. Let us define the angular momentum operators  $L_{\mathbf{r},a}$  and the operators  $K_{\mathbf{r},a}$  and  $N_{\mathbf{r},a}$  by

$$\begin{aligned} L_{\mathbf{r},a} &:= -\epsilon_{abc}m_{\mathbf{r},b}\frac{\partial}{\partial m_{\mathbf{r},c}}, \\ K_{\mathbf{r},a} &:= \epsilon_{abc}L_{\mathbf{r},b}m_{\mathbf{r},c}, \\ N_{\mathbf{r},a} &:= L_{\mathbf{r},a} + \alpha K_{\mathbf{r},a} \end{aligned} \quad (\text{A1})$$

where  $\epsilon_{abc}$  is the totally antisymmetric tensor with rank 3, and  $\alpha$  is the Gilbert damping in Eq. (51). These operators satisfy the following commutation relations:

$$\begin{aligned} [L_{\mathbf{r},a}, L_{\mathbf{r}',b}] &= \delta_{\mathbf{r},\mathbf{r}'}\epsilon_{abc}L_{\mathbf{r},c}, \\ [K_{\mathbf{r},a}, K_{\mathbf{r}',b}] &= -\delta_{\mathbf{r},\mathbf{r}'}\epsilon_{abc}K_{\mathbf{r},c}, \\ [L_{\mathbf{r},a}, K_{\mathbf{r}',b}] &= \delta_{\mathbf{r},\mathbf{r}'}\epsilon_{abc}L_{\mathbf{r},c}, \\ [N_{\mathbf{r},a}, N_{\mathbf{r}',b}] &= \delta_{\mathbf{r},\mathbf{r}'}\{\epsilon_{abc}N_{\mathbf{r},c} + \alpha(N_{\mathbf{r},a}m_{\mathbf{r},b} - m_{\mathbf{r},a}N_{\mathbf{r},b})\}, \end{aligned} \quad (\text{A2})$$

Consider the commutator between the operators  $\mathcal{L}_\alpha := -\sum_{\mathbf{r}} \text{div}[\mathbf{f}_{\mathbf{r},\alpha} \cdot \ ]$  and  $\mathcal{L}_\beta := -\sum_{\mathbf{r}} \text{div}[\mathbf{f}_{\mathbf{r},\beta} \cdot \ ]$ , where  $\mathbf{f}_{\mathbf{r},\gamma}$  ( $\gamma = A, B$ ) is given by

$$\mathbf{f}_{\mathbf{r},\gamma} = -\frac{m_{\mathbf{r}}}{1 + \alpha^2} \times \left( \mathbf{H}_{\mathbf{r},\gamma} + \frac{\alpha}{m_s} \mathbf{m}_{\mathbf{r}} \times \mathbf{H}_{\mathbf{r},\gamma} \right). \quad (\text{A3})$$

From the equation

$$\begin{aligned} \frac{\partial}{\partial m_a} (\epsilon_{abc}m_{\mathbf{r},b}\mathbf{H}_{\mathbf{r},c}) &= -\epsilon_{abc}m_{\mathbf{r},a}\frac{\partial}{\partial m_{\mathbf{r},b}} (\mathbf{H}_{\mathbf{r},\gamma,c}) \\ &= \mathbf{L}_{\mathbf{r}} \cdot \mathbf{H}_{\mathbf{r},\gamma}, \end{aligned} \quad (\text{A4})$$

we can rewrite  $\mathcal{L}_\gamma$  in terms of  $N_{\mathbf{r}}$  as follows:

$$\mathcal{L}_\gamma = \sum_{\mathbf{r}} (\mathbf{L}_{\mathbf{r}} \cdot \bar{\mathbf{H}}_{\mathbf{r},\gamma} + \alpha \mathbf{K}_{\mathbf{r}} \cdot \bar{\mathbf{H}}_{\mathbf{r},\gamma}) = \sum_{\mathbf{r}} N_{\mathbf{r}} \cdot \bar{\mathbf{H}}_{\mathbf{r},\gamma}, \quad (\text{A5})$$

where  $\bar{\mathbf{H}}_{\mathbf{r},\gamma} = \mathbf{H}_{\mathbf{r},\gamma}/(1+\alpha^2)$ . Using Eq. (A2), we obtain

$$[\mathcal{L}_A, \mathcal{L}_B] = \sum_{\mathbf{r}} N_{\mathbf{r}} [\bar{\mathbf{H}}_A, \bar{\mathbf{H}}_B]_{\mathbf{r},\text{mag}}, \quad (\text{A6})$$

where commutator  $[\bar{\mathbf{H}}_A, \bar{\mathbf{H}}_B]_{\mathbf{r},\text{mag}}$  is defined by

$$\begin{aligned} & [\bar{\mathbf{H}}_A, \bar{\mathbf{H}}_B]_{\mathbf{r},\text{mag}} \\ & := \bar{\mathbf{H}}_{\mathbf{r},A} \times \bar{\mathbf{H}}_{\mathbf{r},B} + \frac{\alpha \mathbf{m}_{\mathbf{r}}}{m_s} \times (\bar{\mathbf{H}}_{\mathbf{r},A} \times \bar{\mathbf{H}}_{\mathbf{r},B}) \\ & + \sum_{\mathbf{r}'} [(\bar{\mathbf{H}}_{\mathbf{r}',A} \cdot \mathbf{L}_{\mathbf{r}'}) \bar{\mathbf{H}}_{\mathbf{r},B} - (\bar{\mathbf{H}}_{\mathbf{r}',B} \cdot \mathbf{L}_{\mathbf{r}'}) \bar{\mathbf{H}}_{\mathbf{r},A}] \\ & + \frac{\alpha}{m_s} \sum_{\mathbf{r}'} [(\mathbf{m}_{\mathbf{r}'} \cdot \bar{\mathbf{H}}_{\mathbf{r}',A} \times \mathbf{L}_{\mathbf{r}'}) \bar{\mathbf{H}}_{\mathbf{r},B} - \\ & (\mathbf{m}_{\mathbf{r}'} \cdot \bar{\mathbf{H}}_{\mathbf{r}',B} \times \mathbf{L}_{\mathbf{r}'}) \bar{\mathbf{H}}_{\mathbf{r},A}]. \end{aligned} \quad (\text{A7})$$

Thus,  $[\mathcal{L}_A, \mathcal{L}_B]$  defines the drift field with magnetic field  $[\bar{\mathbf{H}}_A, \bar{\mathbf{H}}_B]_{\mathbf{r},\text{mag}}$ . For example, when  $\mathbf{H}_{\mathbf{r},A} = \mathbf{B}_{-1}$  and  $\mathbf{H}_{\mathbf{r},B} = \mathbf{B}_{+1}$ , we obtain

$$\begin{aligned} [\bar{\mathbf{H}}_A, \bar{\mathbf{H}}_B]_{\mathbf{r},\text{mag}} &= \frac{\mathbf{B}_{-1} \times \mathbf{B}_{+1}}{(1+\alpha^2)\omega} + \frac{\alpha \mathbf{m}_{\mathbf{r}}}{m_s} \times \frac{\mathbf{B}_{-1} \times \mathbf{B}_{+1}}{(1+\alpha^2)\omega} \\ &= \mathbf{b}^{(1)} + \frac{\alpha \mathbf{m}_{\mathbf{r}}}{m_s} \times \mathbf{b}^{(1)}. \end{aligned} \quad (\text{A8})$$

Therefore, from the first-order FM expansion, we obtain

$$\mathcal{L}_F^{(1)} := \sum_{\mathbf{r}} \mathbf{L}_{\mathbf{r}} \cdot \left( \mathbf{b}^{(1)} + \frac{\alpha \mathbf{m}_{\mathbf{r}}}{m_s} \times \mathbf{b}^{(1)} \right), \quad (\text{A9})$$

which gives Eq. (58).

## 2. Two-dimensional ferromagnet: second order

The second-order FM expansion  $\mathcal{L}_F^{(2)}$  is given by

$$\mathcal{L}_F^{(2)} = -\frac{[\mathcal{L}_{-1} [\mathcal{L}_0, \mathcal{L}_1]] + [\mathcal{L}_1 [\mathcal{L}_0, \mathcal{L}_{-1}]]}{2\omega^2}. \quad (\text{A10})$$

We decompose  $\mathcal{L}_0$  into the terms on external field, the nearest-neighbor interaction, and diffusion:

$$\begin{aligned} \mathcal{L}_0^{\text{ext}} &= \frac{1}{1+\alpha^2} \sum_{\mathbf{r}} \mathbf{L}_{\mathbf{r}} \cdot \mathbf{B}_0, \\ \mathcal{L}_0^{\text{int}} &= \frac{J}{1+\alpha^2} \sum_{\mathbf{r}} \mathbf{L}_{\mathbf{r}} \cdot \sum_{\mathbf{r}':n,n} \mathbf{m}_{\mathbf{r}'}, \\ \mathcal{L}_0^{\text{dif}} &= \text{div}_2 (\mathcal{D} \cdot), \end{aligned} \quad (\text{A11})$$

and decompose  $\mathcal{L}_F^{(2)}$  accordingly:  $\mathcal{L}_F^{(2)} = \mathcal{L}_F^{(2),\text{ext}} + \mathcal{L}_F^{(2),\text{int}} + \mathcal{L}_F^{(2),\text{dif}}$ . Combining Eqs. (A7) and (A11), we

obtain

$$\begin{aligned} \mathcal{L}_F^{(2),\text{ext}} &= \sum_{\mathbf{r}} \mathbf{L}_{\mathbf{r}} \cdot \left( (1-\alpha^2) \mathbf{b}^{(2)} + \frac{2\alpha \mathbf{m}_{\mathbf{r}}}{m_s} \times \mathbf{b}^{(2)} \right), \\ \mathcal{L}_F^{(2),\text{int}} &= \sum_{\mathbf{r}} \mathbf{L}_{\mathbf{r}} \cdot J \left( \frac{\alpha B_d}{m_s \omega (1+\alpha^2)} \right)^2 \mathbf{m}_{\mathbf{r}',z} \\ &\quad \times \sum_{\mathbf{r}':n,n} \begin{pmatrix} m_{\mathbf{r}',x} \delta m_{\mathbf{r},\mathbf{r}',z} \\ m_{\mathbf{r}',y} \delta m_{\mathbf{r},\mathbf{r}',z} \\ -m_{\mathbf{r}',z} \delta m_{\mathbf{r},\mathbf{r}',x} - m_{\mathbf{r}',y} \delta m_{\mathbf{r},\mathbf{r}',y} \end{pmatrix} \\ &= \sum_{\mathbf{r}} \mathbf{L}_{\mathbf{r}} \cdot \sum_{\mathbf{r}':n,n} \delta \mathbf{J}_{\mathbf{r},\mathbf{r}'}, \\ \mathcal{L}_F^{(2),\text{dif}} &= \text{div} \left[ \left( \frac{2\chi_{\mathbf{r}}}{1+\alpha^2} \mathbf{m}_{\mathbf{r}} \right) \cdot \right] + \text{div}_2 [\chi_{\mathbf{r}} DGG^{\text{tr}} \cdot], \end{aligned} \quad (\text{A12})$$

where  $\delta \mathbf{m}_{\mathbf{r},\mathbf{r}'} = \mathbf{m}_{\mathbf{r}} - \mathbf{m}_{\mathbf{r}'}$ . The overall effective master equation is given by

$$\begin{aligned} \partial_t P &= \sum_{\mathbf{r}} (\mathbf{L}_{\mathbf{r}} \cdot \widetilde{\mathbf{H}}_{F,\mathbf{r}} P) + \text{div} \left[ \left( \frac{2(1+\chi)}{1+\alpha^2} \mathbf{m}_{\mathbf{r}} \right) P \right] \\ &\quad + \text{div}_2 [(1+\chi) DGG^{\text{tr}} P], \end{aligned} \quad (\text{A13})$$

where the effective field  $\widetilde{\mathbf{H}}_{F,\mathbf{r}}$  is

$$\begin{aligned} \widetilde{\mathbf{H}}_{F,\mathbf{r}} &= \sum_{\mathbf{r}':n,n} (J \mathbf{m}_{\mathbf{r}'} + \delta \mathbf{J}_{\mathbf{r},\mathbf{r}'}) + \mathbf{B}_0 + \mathbf{b}^{(1)} + (1-\alpha^2) \mathbf{b}^{(2)} \\ &\quad + \left( -\frac{\alpha}{m_s} \mathbf{b}^{(1)} - \frac{2\alpha}{m_s} \mathbf{b}^{(2)} \right) \times \mathbf{m}_{\mathbf{r}}. \end{aligned} \quad (\text{A14})$$

By defining a new diffusion matrix  $G_F$  by  $G_F := (1+\chi)^{1/2} G$ , the second and third terms in Eq. (A13) are rewritten as

$$\begin{aligned} & \text{div} \left[ \left( \frac{2(1+\chi)}{1+\alpha^2} \mathbf{m}_{\mathbf{r}} \right) P \right] \\ &= \sum_{\mathbf{r}} \mathbf{L}_{\mathbf{r}} \cdot \left( -\mathbf{b}^{(2),\text{dif}} + \frac{\mathbf{b}^{(2),\text{dif}}}{m_s} \times \mathbf{m}_{\mathbf{r}} \right) P \\ &\quad + \text{div} (-\mathbf{d}_F P), \\ & \text{div}_2 [(1+\chi) DGG^{\text{tr}} P] = \text{div}_2 [DG_F G_F^{\text{tr}} P], \end{aligned} \quad (\text{A15})$$

where  $\mathbf{d}_{F,i} := g_{F,kl} \partial_k g_{F,il}$  and

$$\mathbf{b}^{(2),\text{dif}} := \frac{Dm_s}{2(1+\alpha^2)} \frac{\delta \chi_{\mathbf{r}}}{\delta \mathbf{m}_{\mathbf{r}}}. \quad (\text{A16})$$

Equation (A13) is then rewritten as

$$\begin{aligned} \partial_t P &= \sum_{\mathbf{r}} (\mathbf{L}_{\mathbf{r}} \cdot \mathbf{H}_{F,\mathbf{r}} P) + \text{div} (-\mathbf{d}_F P) \\ &\quad + \text{div}_2 [DG_F G_F^{\text{tr}} P], \end{aligned} \quad (\text{A17})$$

where  $\mathbf{H}_{F,\mathbf{r}}$  is the effective field defined in Eq. (63). Comparing this equation with Eq. (10), we finally arrive at the sLLG equation (62).



### 3. Multiferroic spin chain

When we perform the FM expansion of the sLLG equation for the multiferroic spin chain model (67), the calculation is done in a similar manner to App. A 1. The first-order Fokker-Planck operator  $\mathcal{L}_F^{(1)}$  is given by

$$\mathcal{L}_F^{(1)} := \sum_{\mathbf{r}} \mathbf{L}_{\mathbf{r}} \cdot \frac{i}{\omega} [\bar{\mathbf{H}}_{-1}, \bar{\mathbf{H}}_1]_{\mathbf{r}, \text{mag}}, \quad (\text{A18})$$

where the Fourier harmonics  $\bar{\mathbf{H}}_{\pm 1}$  of the effective field is

$$\begin{aligned} \bar{\mathbf{H}}_{\pm 1} &:= \sum_{\mathbf{r}': n.n.} \mathbf{D}_{\pm} \times \mathbf{m}_{\mathbf{r}'} + \mathbf{B}_{\pm}, \\ \mathbf{D}_{\pm} &:= \frac{g_{me} E_d}{2} \begin{pmatrix} \pm i \\ 1 \\ 0 \end{pmatrix}, \\ \mathbf{B}_{\pm} &:= \frac{B_d}{2} \begin{pmatrix} 1 \\ \mp i \\ 0 \end{pmatrix}. \end{aligned} \quad (\text{A19})$$

By a straightforward calculation, we obtain

$$\begin{aligned} \mathcal{L}_F^{(1)} &:= \sum_{\mathbf{r}} \mathbf{L}_{\mathbf{r}} \cdot \mathbf{H}_{F, \mathbf{r}}^{(1)}, \\ \mathbf{H}_{F, \mathbf{r}}^{(1)} &:= \sum_{\mathbf{r}': n.n.} (\mathbf{D}_{F, \mathbf{r}, \mathbf{r}'} \times \mathbf{m}_{\mathbf{r}'}) + \mathbf{B}_F - \alpha \mathbf{B}_F \times \mathbf{m}_{\mathbf{r}} \\ &\quad - \sum_{\mathbf{r}': n.n.} \frac{\alpha \epsilon_B \epsilon_E}{2m_s(1 + \alpha^2)\omega} \begin{pmatrix} m_s^2 + m_{\mathbf{r}', y} \delta m_{\mathbf{r}, y} \\ -m_{\mathbf{r}', y} \delta m_{\mathbf{r}, x} \\ 0 \end{pmatrix}, \end{aligned} \quad (\text{A20})$$

where  $\mathbf{D}_{F, \mathbf{r}, \mathbf{r}'}$  and  $\mathbf{B}_F$  are defined in Eq. (71). This equation follows from the correspondence between a master equation and an EOM.

- 
- [1] A. Kirilyuk, A. V. Kimel, and T. Rasing, *Rev. Mod. Phys.* **82**, 2731 (2010).
  - [2] M. Bukov, L. D'Alessio, and A. Polkovnikov, *Advances in Physics* **64**, 139 (2015).
  - [3] A. Eckardt, *Rev. Mod. Phys.* **89**, 11004 (2017).
  - [4] T. Oka and S. Kitamura, *arXiv preprint arXiv:1804.03212* (2018).
  - [5] R. Matsunaga, Y. I. Hamada, K. Makise, Y. Uzawa, H. Terai, Z. Wang, and R. Shimano, *Phys. Rev. Lett.* **111**, 57002 (2013).
  - [6] R. Matsunaga, N. Tsuji, H. Fujita, A. Sugioka, K. Makise, Y. Uzawa, H. Terai, Z. Wang, H. Aoki, and R. Shimano, *Science* **345**, 1145 (2014).
  - [7] K. Katsumi, N. Tsuji, Y. I. Hamada, R. Matsunaga, J. Schneeloch, R. D. Zhong, G. D. Gu, H. Aoki, Y. Gallais, and R. Shimano, *Physical review letters* **120**, 117001 (2018).
  - [8] D. H. Dunlap and V. M. Kenkre, *Phys. Rev. B* **34**, 3625 (1986).
  - [9] H. Lignier, C. Sias, D. Ciampini, Y. Singh, A. Zenesini, O. Morsch, and E. Arimondo, *Phys. Rev. Lett.* **99**, 220403 (2007).
  - [10] M. Grifoni and P. Hänggi, *Physics Reports* **304**, 229 (1998).
  - [11] F. Grossmann, T. Dittrich, P. Jung, and P. Hänggi, *Phys. Rev. Lett.* **67**, 516 (1991).
  - [12] C. Chicone, *Ordinary differential equations with applications*, Vol. 34 (Springer Science & Business Media, 2006).
  - [13] A. Eckardt, C. Weiss, and M. Holthaus, *Phys. Rev. Lett.* **95**, 260404 (2005).
  - [14] A. Eckardt, M. Holthaus, H. Lignier, A. Zenesini, D. Ciampini, O. Morsch, and E. Arimondo, *Phys. Rev. A* **79**, 13611 (2009).
  - [15] A. Zenesini, H. Lignier, D. Ciampini, O. Morsch, and E. Arimondo, *Phys. Rev. Lett.* **102**, 100403 (2009).
  - [16] D. Jaksch and P. Zoller, *New Journal of Physics* **5**, 56 (2003).
  - [17] M. Aidelsburger, M. Atala, M. Lohse, J. T. Barreiro, B. Paredes, and I. Bloch, *Phys. Rev. Lett.* **111**, 185301 (2013).
  - [18] M. Aidelsburger, M. Lohse, C. Schweizer, M. Atala, J. T. Barreiro, S. Nascimbène, N. R. Cooper, I. Bloch, and N. Goldman, *Nature Physics* **11**, 162 (2014).
  - [19] C. J. Kennedy, W. C. Burton, W. C. Chung, and W. Ketterle, *Nature Physics* **11**, 859 (2015).
  - [20] J. Struck, C. Ölschläger, R. Le Targat, P. Soltan-Panahi, A. Eckardt, M. Lewenstein, P. Windpassinger, and K. Sengstock, *Science* **333**, 996 (2011).
  - [21] J. Struck, M. Weinberg, C. Ölschläger, P. Windpassinger, J. Simonet, K. Sengstock, R. Höppner, P. Hauke, A. Eckardt, M. Lewenstein, and L. Mathey, *Nature Physics* **9**, 738 (2013).
  - [22] F. Görg, M. Messer, K. Sandholzer, G. Jotzu, R. Desbuquois, and T. Esslinger, *Nature* **553**, 481 (2018).
  - [23] T. Oka and H. Aoki, *Phys. Rev. B* **79**, 81406 (2009).
  - [24] T. Kitagawa, E. Berg, M. Rudner, and E. Demler, *Phys. Rev. B* **82**, 235114 (2010).
  - [25] N. H. Lindner, G. Refael, and V. Galitski, *Nature Physics* **7**, 490 (2011).

- [26] Y. H. Wang, H. Steinberg, P. Jarillo-Herrero, and N. Gedik, *Science* **342**, 453 (2013).
- [27] G. Jotzu, M. Messer, R. Desbuquois, M. Lebrat, T. Uehlinger, D. Greif, and T. Esslinger, *Nature* **515**, 237 (2014).
- [28] M. C. Rechtsman, J. M. Zeuner, Y. Plotnik, Y. Lumer, D. Podolsky, F. Dreisow, S. Nolte, M. Segev, and A. Szameit, *Nature* **496**, 196 (2013).
- [29] M. Sato, Y. Sasaki, and T. Oka, arXiv preprint arXiv:1404.2010 (2014).
- [30] S. Takayoshi, H. Aoki, and T. Oka, *Phys. Rev. B* **90**, 85150 (2014).
- [31] S. Takayoshi, M. Sato, and T. Oka, *Phys. Rev. B* **90**, 214413 (2014).
- [32] M. Sato, S. Takayoshi, and T. Oka, *Phys. Rev. Lett.* **117**, 147202 (2016).
- [33] J. H. Mentink, K. Balzer, and M. Eckstein, *Nature Communications* **6**, 6708 (2015).
- [34] N. Goldman and J. Dalibard, *Phys. Rev. X* **4**, 31027 (2014).
- [35] S. Rahav, I. Gilary, and S. Fishman, *Phys. Rev. A* **68**, 13820 (2003).
- [36] A. Eckardt and E. Anisimovas, *New Journal of Physics* **17**, 93039 (2015).
- [37] T. Kuwahara, T. Mori, and K. Saito, *Annals of Physics* **367**, 96 (2016), arXiv:1508.05797.
- [38] T. Mori, T. Kuwahara, and K. Saito, *Phys. Rev. Lett.* **116**, 120401 (2016).
- [39] D. A. Abanin, W. De Roeck, W. W. Ho, and F. b. ç. Huvneers, *Phys. Rev. B* **95**, 14112 (2017).
- [40] L. D'Alessio and A. Polkovnikov, *Annals of Physics* **333**, 19 (2013).
- [41] L. D'Alessio and M. Rigol, *Phys. Rev. X* **4**, 41048 (2014).
- [42] P. Ponte, A. Chandran, Z. Papić, and D. A. Abanin, *Annals of Physics* **353**, 196 (2015).
- [43] A. Lazarides, A. Das, and R. Moessner, *Phys. Rev. E* **90**, 12110 (2014).
- [44] D. J. Luitz, Y. B. Lev, and A. Lazarides, *SciPost Phys.* **3**, 29 (2017).
- [45] O. Howell, P. Weinberg, D. Sels, A. Polkovnikov, and M. Bukov, arXiv preprint arXiv:1802.04910 (2018).
- [46] T. Mori, *Phys. Rev. B* **98**, 104303 (2018), arXiv:arXiv preprint arXiv:1804.02165.
- [47] B. V. Chirikov, F. M. Izrailev, and D. L. Shepelyansky, *Mathematical physics reviews* **2**, 209 (1981).
- [48] L. Gammatoni, P. Hänggi, P. Jung, and F. Marchesoni, *Rev. Mod. Phys.* **70**, 223 (1998).
- [49] P. Jung, *Physics Reports* **234**, 175 (1993).
- [50] P. L. Kapitza, *Soviet Physics-JETP* **21**, 588 (1951).
- [51] W. Paul, *Rev. Mod. Phys.* **62**, 531 (1990).
- [52] E. D. Courant, M. S. Livingston, and H. S. Snyder, *Phys. Rev.* **88**, 1190 (1952).
- [53] R. P. Feynman, Reading, Ma.: Addison-Wesley, 1964, edited by Feynman, Richard P.; Leighton, Robert B.; Sands, Matthew (1964).
- [54] H. Saito and M. Ueda, *Phys. Rev. Lett.* **90**, 40403 (2003).
- [55] F. K. Abdullaev, J. G. Caputo, R. A. Kraenkel, and B. A. Malomed, *Phys. Rev. A* **67**, 13605 (2003).
- [56] N. G. Van Kampen, *Stochastic processes in physics and chemistry*, Vol. 1 (Elsevier, 1992).
- [57] C. J. Pethick and H. Smith, *Bose-Einstein condensation in dilute gases* (Cambridge university press, Cambridge, 2002).
- [58] D. M. Stamper-Kurn and M. Ueda, *Reviews of Modern Physics* **85**, 1191 (2013).
- [59] L. Landau and E. Lifshitz, *Phys. Z. Sowjetunion* **8**, 101 (1935).
- [60] T. L. Gilbert, *IEEE Transactions on Magnetism* **40**, 3443 (2004).
- [61] W. F. Brown, *Phys. Rev.* **130**, 1677 (1963).
- [62] W. Kohn, *Journal of Statistical Physics* **103**, 417 (2001).
- [63] D. W. Hone, R. Ketzmerick, and W. Kohn, *Phys. Rev. E* **79**, 51129 (2009).
- [64] R. Ketzmerick and W. Wustmann, *Phys. Rev. E* **82**, 21114 (2010).
- [65] M. Langemeyer and M. Holthaus, *Phys. Rev. E* **89**, 12101 (2014).
- [66] T. Iadecola, T. Neupert, and C. Chamon, *Phys. Rev. B* **91**, 235133 (2015).
- [67] H. Dehghani, T. Oka, and A. Mitra, *Phys. Rev. B* **90**, 195429 (2014).
- [68] K. I. Seetharam, C.-E. Bardyn, N. H. Lindner, M. S. Rudner, and G. Refael, *Phys. Rev. X* **5**, 41050 (2015).
- [69] D. Vorberg, W. Wustmann, R. Ketzmerick, and A. Eckardt, *Phys. Rev. Lett.* **111**, 240405 (2013).
- [70] D. Vorberg, W. Wustmann, H. Schomerus, R. Ketzmerick, and A. Eckardt, *Phys. Rev. E* **92**, 62119 (2015).
- [71] Y. Wan and R. Moessner, arXiv preprint arXiv:1808.02044 (2018).
- [72] H. Risken, in *The Fokker-Planck Equation* (Springer, 1996) pp. 63–95.
- [73] S. Maekawa, S. O. Valenzuela, T. Kimura, and E. Saitoh, eds., *Spin current* (Oxford University Press, 2017).
- [74] T. Moriya, *Phys. Rev.* **120**, 91 (1960).
- [75] I. Dzyaloshinsky, *Journal of Physics and Chemistry of Solids* **4**, 241 (1958).
- [76] M. V. Moreno, Z. G. Arenas, and D. G. Barci, *Phys. Rev. E* **91**, 42103 (2015).
- [77] I. D. Mayergoyz, G. Bertotti, and C. Serpico, *Nonlinear magnetization dynamics in nanosystems* (Elsevier, 2009).
- [78] P. C. Hohenberg and A. P. Krekhov, *Physics Reports* **572**, 1 (2015).
- [79] M. J. Bhaseen, J. Mayoh, B. D. Simons, and J. Keeling, *Phys. Rev. A* **85**, 13817 (2012).
- [80] L. Bakemeier, A. Alvermann, and H. Fehske, *Phys. Rev. A* **88**, 43835 (2013).
- [81] W. T. Coffey and Y. P. Kalmykov, *The Langevin equation: with applications to stochastic problems in physics, chemistry and electrical engineering* (World Scientific, 2004).
- [82] J. L. Garcia-Palacios and F. J. Lázaro, *Phys. Rev. B* **58**, 14937 (1998).
- [83] K. Kanazawa, T. Sagawa, and H. Hayakawa, *Phys. Rev. Lett.* **108**, 210601 (2012).
- [84] K. Kanazawa, T. Sagawa, and H. Hayakawa, *Phys. Rev. E* **87**, 52124 (2013).
- [85] R. Zwanzig, *Physical Review* **124**, 983 (1961).
- [86] H. Mori and H. Fujisaka, *Progress of Theoretical Physics* **49**, 764 (1973).
- [87] F. Haake, in *Springer tracts in modern physics* (Springer, 1973) pp. 98–168.
- [88] H. Hinrichsen, *Advances in Physics* **49**, 815 (2000).
- [89] D. Prato and P. W. Lamberti, *The Journal of Chemical Physics* **106**, 4640 (1997).

- [90] I. Bialynicki-Birula, B. Mielnik, and J. Plebański, *Annals of Physics* **51**, 187 (1969).
- [91] E. S. Mananga and T. Charpentier, *The Journal of Chemical Physics* **135**, 44109 (2011).
- [92] T. Mikami, S. Kitamura, K. Yasuda, N. Tsuji, T. Oka, and H. Aoki, *Phys. Rev. B* **93**, 144307 (2016).
- [93] M. Bukov, M. Kolodrubetz, and A. Polkovnikov, *Phys. Rev. Lett.* **116**, 125301 (2016).
- [94] S. Kitamura, T. Oka, and H. Aoki, *Phys. Rev. B* **96**, 14406 (2017).
- [95] M. Claassen, H.-C. Jiang, B. Moritz, and T. P. Devereaux, *Nature Communications* **8**, 1192 (2017).
- [96] Schnell Alexander, E. André, and D. Sergey, arXiv preprint arXiv:1809.11121 (2018).
- [97] K. Kanazawa, T. G. Sano, T. Sagawa, and H. Hayakawa, *Journal of Statistical Physics* **160**, 1294 (2015).
- [98] S. Blanes, F. Casas, J. A. Oteo, and J. Ros, *Physics Reports* **470**, 151 (2009).
- [99] F. Spirig, *Celestial mechanics* **20**, 343 (1979).
- [100] A. A. Agrachev and R. V. Gamkrelidze, *Journal of Soviet Mathematics* **17**, 1650 (1981).
- [101] A. A. A. Gamkrelidze and R. V., *Mathematics of the USSR-Sbornik* **35**, 727 (1979).
- [102] J. A. O. Ros and J., *Journal of Physics A: Mathematical and General* **24**, 5751 (1991).
- [103] S. Tani, *American Journal of Physics* **36**, 29 (1968).
- [104] R. A. Marcus, *The Journal of Chemical Physics* **52**, 4803 (1970).
- [105] G. Casati, I. Guarneri, and G. Mantica, *Phys. Rev. A* **50**, 5018 (1994).
- [106] H. Wiedemann, J. Mostowski, and F. Haake, *Phys. Rev. A* **49**, 1171 (1994).
- [107] C. O. Reinhold, J. Burgdörfer, M. T. Frey, and F. B. Dunning, *Phys. Rev. Lett.* **79**, 5226 (1997).
- [108] E. Beaupaire, J.-C. Merle, A. Daunois, and J.-Y. Bigot, *Phys. Rev. Lett.* **76**, 4250 (1996).
- [109] U. Atxitia, O. Chubykalo-Fesenko, R. W. Chantrell, U. Nowak, and A. Rebei, *Phys. Rev. Lett.* **102**, 57203 (2009).
- [110] N. Kazantseva, U. Nowak, R. W. Chantrell, J. Hohlfeld, and A. Rebei, *EPL (Europhysics Letters)* **81**, 27004 (2008).
- [111] Z. Li and S. Zhang, *Phys. Rev. B* **69**, 134416 (2004).
- [112] C. Aron, D. G. Barci, L. F. Cugliandolo, Z. G. Arenas, and G. S. Lozano, *Journal of Statistical Mechanics: Theory and Experiment* **2014**, P09008 (2014).
- [113] J. C. Slonczewski, *Journal of Magnetism and Magnetic Materials* **159**, L1 (1996).
- [114] L. Berger, *Phys. Rev. B* **54**, 9353 (1996).
- [115] M. Tsoi, A. G. M. Jansen, J. Bass, W.-C. Chiang, M. Seck, V. Tsoi, and P. Wyder, *Phys. Rev. Lett.* **80**, 4281 (1998).
- [116] E. B. Myers, D. C. Ralph, J. A. Katine, R. N. Louie, and R. A. Buhrman, *Science* **285**, 867 (1999).
- [117] S. Seki and M. Mochizuki, *Skyrmions in magnetic materials* (Springer, 2016).
- [118] F. Haddadfarshi, J. Cui, and F. Mintert, *Phys. Rev. Lett.* **114**, 130402 (2015).
- [119] T. Shirai, J. Thingna, T. Mori, S. Denisov, P. Hänggi, and S. Miyashita, *New Journal of Physics* **18**, 53008 (2016).
- [120] C. M. Dai, Z. C. Shi, and X. X. Yi, *Phys. Rev. A* **93**, 32121 (2016).
- [121] C. M. Dai, H. Li, W. Wang, and X. X. Yi, arXiv preprint arXiv:1707.05030 (2017).
- [122] Y. Tokura, S. Seki, and N. Nagaosa, *Reports on Progress in Physics* **77**, 76501 (2014).
- [123] K. F. Wang, J.-M. Liu, and Z. F. Ren, *Advances in Physics* **58**, 321 (2009).
- [124] H. Katsura, N. Nagaosa, and A. V. Balatsky, *Phys. Rev. Lett.* **95**, 57205 (2005).
- [125] H. Katsura, A. V. Balatsky, and N. Nagaosa, *Phys. Rev. Lett.* **98**, 27203 (2007).
- [126] I. A. Sergienko and E. Dagotto, *Phys. Rev. B* **73**, 94434 (2006).
- [127] M. Mostovoy, *Phys. Rev. Lett.* **96**, 67601 (2006).
- [128] T. Miyadai, K. Kikuchi, H. Kondo, S. Sakka, M. Arai, and Y. Ishikawa, *Journal of the Physical Society of Japan* **52**, 1394 (1983).
- [129] M. Shinozaki, S. Hoshino, Y. Masaki, J.-i. Kishine, and Y. Kato, *Journal of the Physical Society of Japan* **85**, 74710 (2016).
- [130] H. Hirori, K. Shinokita, M. Shirai, S. Tani, Y. Kadoya, and K. Tanaka, *Nature Communications* **2**, 594 (2011).
- [131] A. Pashkin, F. Junginger, B. Mayer, C. Schmidt, O. Schubert, D. Brida, R. Huber, and A. Leitenstorfer, *IEEE Journal of Selected Topics in Quantum Electronics* **19**, 8401608 (2013).
- [132] Y. Takahashi, R. Shimano, Y. Kaneko, H. Murakawa, and Y. Tokura, *Nature Physics* **8**, 121 (2011).
- [133] D. Hüvonen, U. Nagel, T. Rööm, Y. J. Choi, C. L. Zhang, S. Park, and S.-W. Cheong, *Phys. Rev. B* **80**, 100402 (2009).
- [134] S. Furukawa, M. Sato, and S. Onoda, *Phys. Rev. Lett.* **105**, 257205 (2010).
- [135] J.-i. Kishine, K. Inoue, and Y. Yoshida, *Progress of Theoretical Physics Supplement* **159**, 82 (2005).
- [136] Y. Togawa, Y. Kousaka, S. Nishihara, K. Inoue, J. Akimitsu, A. S. Ovchinnikov, and J. Kishine, *Phys. Rev. Lett.* **111**, 197204 (2013).
- [137] C. E. Rüter, K. G. Makris, R. El-Ganainy, D. N. Christodoulides, M. Segev, and D. Kip, *Nature Physics* **6**, 192 (2010).
- [138] Y. C. Hu and T. L. Hughes, *Phys. Rev. B* **84**, 153101 (2011).
- [139] H. Schomerus, *Opt. Lett.* **38**, 1912 (2013).
- [140] G. Barontini, R. Labouvie, F. Stubenrauch, A. Vogler, V. Guarrera, and H. Ott, *Phys. Rev. Lett.* **110**, 35302 (2013).
- [141] S. Malzard, C. Poli, and H. Schomerus, *Phys. Rev. Lett.* **115**, 200402 (2015).
- [142] H. Cao and J. Wiersig, *Rev. Mod. Phys.* **87**, 61 (2015).
- [143] T. E. Lee, *Phys. Rev. Lett.* **116**, 133903 (2016).
- [144] P. Peng, W. Cao, C. Shen, W. Qu, J. Wen, L. Jiang, and Y. Xiao, *Nature Physics* **12**, 1139 (2016).
- [145] B. Peng, b. S. K. Özdemir, M. Liertzer, W. Chen, J. Kramer, H. Yılmaz, J. Wiersig, S. Rotter, and L. Yang, *Proceedings of the National Academy of Sciences* **113**, 6845 (2016).
- [146] W. Chen, . Kaya Özdemir, G. Zhao, J. Wiersig, and L. Yang, *Nature* **548**, 192 (2017).
- [147] D. Leykam, K. Y. Bliokh, C. Huang, Y. D. Chong, and F. Nori, *Phys. Rev. Lett.* **118**, 40401 (2017).
- [148] Y. Xu, S.-T. Wang, and L.-M. Duan, *Phys. Rev. Lett.* **118**, 45701 (2017).

- [149] H. Zhou, C. Peng, Y. Yoon, C. W. Hsu, K. A. Nelson, L. Fu, J. D. Joannopoulos, M. Soljačić, and B. Zhen, *Science* **359**, 1009 (2018).
- [150] M. A. Bandres, S. Wittek, G. Harari, M. Parto, J. Ren, M. Segev, D. N. Christodoulides, and M. Khajavikhan, *Science* **359** (2018), 10.1126/science.aar4005.
- [151] Z. Gong, Y. Ashida, K. Kawabata, K. Takasan, S. Higashikawa, and M. Ueda, *Phys. Rev. X* **8**, 031079 (2018), arXiv:arXiv preprint arXiv:1802.07964.
- [152] K. Kawabata, S. Higashikawa, Z. Gong, Y. Ashida, and M. Ueda, arXiv preprint arXiv:1804.04676 (2018).
- [153] S. Ryu, A. P. Schnyder, A. Furusaki, and A. W. W. Ludwig, *New Journal of Physics* **12** (2010), 10.1088/1367-2630/12/6/065010, arXiv:0912.2157.
- [154] A. P. Schnyder, S. Ryu, A. Furusaki, and A. W. W. Ludwig, *AIP Conference Proceedings* **1134**, 10 (2009), arXiv:0905.2029.
- [155] A. Kitaev, *AIP Conference Proceedings* **1134**, 22 (2009), arXiv:0901.2686.
- [156] L. Jiang, T. Kitagawa, J. Alicea, A. R. Akhmerov, D. Pekker, G. Refael, J. I. Cirac, E. Demler, M. D. Lukin, and P. Zoller, *Phys. Rev. Lett.* **106**, 220402 (2011).
- [157] M. S. Rudner, N. H. Lindner, E. Berg, and M. Levin, *Phys. Rev. X* **3**, 31005 (2013).